



This discussion paper is/has been under review for the journal Biogeosciences (BG).
Please refer to the corresponding final paper in BG if available.

The distribution, dominance patterns and ecological niches of plankton functional types in Dynamic Green Ocean Models and satellite estimates

M. Vogt¹, T. Hashioka^{2,3,4}, M. R. Payne^{1,5}, E. T. Buitenhuis⁶, C. Le Quéré⁷,
S. Alvain⁸, M. N. Aita⁹, L. Bopp¹⁰, S. C. Doney¹¹, T. Hirata², I. Lima¹¹,
S. Saille^{11,*}, and Y. Yamanaka^{2,4}

¹Institute for Biogeochemistry and Pollutant Dynamics, Swiss Federal Institute of Technology, Zurich, Switzerland

²Graduate School of Environmental Earth Science, Hokkaido University, Sapporo, Japan

³Tyndall Centre for Climate Research, University of East Anglia, Norwich, UK

⁴Core Research for Evolutionary Science and Technology, Japanese Science and Technology Agency, Tokyo, Japan

⁵Center for Ocean Life, National Institute of Aquatic Resources (DTU-Aqua), Technical University of Denmark, Charlottenlund, Denmark

⁶School of Environmental Sciences, University of East Anglia, Norwich, UK

⁷Tyndall Centre for Climate Research, University of East Anglia, Norwich, UK

⁸LOG, Université Lille Nord de France, ULCO, CNRS, Wimereux, France

Title Page

Abstract

Introduction

Conclusions

References

Tables

Figures



Back

Close

Full Screen / Esc

Printer-friendly Version

Interactive Discussion



⁹Japanese Agency for Marine-Earth Science and Technology (JAMSTEC), Yokohama, Japan

¹⁰Laboratoire du Climat et de l'Environnement (LSCE), Gif-sur-Yvette, France

¹¹Woods Hole Oceanographic Institution (WHOI), Woods Hole, USA

*now at: Plymouth Marine Laboratory, Plymouth, UK

Received: 10 October 2013 – Accepted: 18 October 2013 – Published: 4 November 2013

Correspondence to: M. Vogt (meike.vogt@env.ethz.ch)

Published by Copernicus Publications on behalf of the European Geosciences Union.

BGD

10, 17193–17247, 2013

Distribution, dominance and ecological niches of PFTs

M. Vogt et al.

Title Page

Abstract

Introduction

Conclusions

References

Tables

Figures



Back

Close

Full Screen / Esc

Printer-friendly Version

Interactive Discussion

Abstract

We compare the spatial and temporal representation of phytoplankton functional types (pPFTs) in four different Dynamic Green Ocean Models (DGOMs; CCSM-BEC, NEMURO, PISCES and PlankTOM5) to derived phytoplankton distributions from two independent satellite estimates, with a particular focus on diatom distributions. Global annual mean surface biomass estimates for diatoms vary between $0.23 \text{ mmol C m}^{-3}$ and $0.77 \text{ mmol C m}^{-3}$ in the models, and are comparable to a satellite-derived estimate ($0.41 \text{ mmol C m}^{-3}$). All models consistently simulate a higher zonal mean diatom biomass contribution in the high latitudes than in the low latitudes, but the relative diatom contribution varies substantially between models with largest differences in the high latitudes (20 % to 100 % of total biomass). We investigate phytoplankton distribution in terms of annual and monthly mean dominance patterns, i.e. the distribution of locations where a given PFT contributes more than 50 % to total biomass. In all models, diatoms tend to dominate large areas of the high latitudes of both hemispheres, and the area of the surface ocean dominated by diatoms is significantly higher in the models than in the satellite estimates. We estimate the realized ecological niches filled by the dominant pPFT at each location as a function of annual mean surface nitrate concentration (NO_3), sea surface temperature (SST), and mixed layer depth. A general additive model (GAM) is used to map the probability of dominance of all pPFTs in niche and geographic space. Models tend to simulate diatom dominance over a wider temperature and nutrient range, whereas satellites confine diatom dominance to a narrower niche of low-intermediate annual mean temperatures (annual mean SST $< 10^\circ\text{C}$), but allow for niches in different ranges of surface NO_3 concentrations. For annual mean diatom dominance, the statistically modelled probability of dominance explains the majority of the variance in the data (65.2–66.6 %). For the satellite estimates, the explained deviance is much lower (44.6 % and 32.7 %). The differences in the representation of diatoms among models and compared to satellite estimates highlights the need to bet-

Distribution, dominance and ecological niches of PFTs

M. Vogt et al.

Title Page

Abstract

Introduction

Conclusions

References

Tables

Figures



Back

Close

Full Screen / Esc

Printer-friendly Version

Interactive Discussion



ter resolve phytoplankton succession and phenology in the models. This work is part of the marine ecosystem inter-comparison project (MAREMIP).

1 Introduction

Marine ecosystems are complex ensembles of interacting species on several trophic levels. On the lowest trophic level, phytoplankton form the base of the marine food web and contribute 50 % of photosynthetic activity on the Earth (Buitenhuis et al., 2013a; Field et al., 1998). Phytoplankton activity influences the marine cycling of micro- and macronutrients (e.g. Weber and Deutsch, 2010, 2012), and the export of organic matter generated in planktic ecosystems is a major sink of atmospheric carbon on glacial-interglacial time-scales (Sigman and Boyle, 2000). Thus, marine ecosystems are influenced by and may feedback to climate and climate change (Doney et al., 2012).

Dynamic Green Ocean Models (DGOMs) are marine ecosystem models based on plankton functional types (PFTs), groups of plankton carrying out a specific function in the ocean (Le Quéré et al., 2005; Iglesias-Rodríguez et al., 2002), such as silicification (diatoms), calcification (coccolithophores) or nitrogen fixation (e.g. *Trichodesmium*). At present, several DGOMs with varying degrees of complexity exist, and they have been widely used to study different aspects of global biogeochemical cycles: models were used to investigate the marine carbon (Bopp et al., 2003) and nitrogen cycles (Moore and Doney, 2007; Moore et al., 2006), the response of marine productivity to future climate change (Steinacher et al., 2010), to simulate the response of ecosystems to iron fertilization (Aumont and Bopp, 2006), to study the ocean biogeochemical response to dust input (Moore et al., 2006), the marine sulphur cycle (Le Clainche et al., 2010; Vogt et al., 2010) or the influence of plankton biomass on the bio-optical properties of the ocean (Mouw et al., 2012; Manizza et al., 2008). Several state-of-the-art DGOMs are included in modern coupled climate models (Anav et al., 2013; Friedlingstein et al., 2006). DGOMs are also used in many regional studies, e.g. to simulate plankton dy-

BGD

10, 17193–17247, 2013

Distribution, dominance and ecological niches of PFTs

M. Vogt et al.

Title Page

Abstract

Introduction

Conclusions

References

Tables

Figures

⏪

⏩

◀

▶

Back

Close

Full Screen / Esc

Printer-friendly Version

Interactive Discussion

namics in the North Sea (Siddorn et al., 2007), the Arctic (Popova et al., 2012) and the Southern Ocean (Wang and Moore, 2011).

In the past, the validation of DGOMs has proven to be difficult, as few observations of biomass or physiological rates for the planktonic community were available (Anderson, 2005). In recent years, however, satellite observations (Alvain et al., 2005, 2008, 2012; Hirata et al., 2011) and pigment estimations (Peloquin et al., 2013; Uitz et al., 2006) as well as in situ observations of plankton abundance and biomass (Buitenhuis et al., 2013b) have become available. Satellite estimates provide global coverage on fine temporal and spatial scales, and are highly promising for long-term monitoring of plankton communities. A multitude of different satellite algorithms exist, with some focussing on single plankton groups (e.g. Balch et al., 1996; Brown and Yoder, 1994; Iglesias-Rodríguez et al., 2002; Smyth et al., 2004; Shutler et al., 2013; Subramaniam and Brown, 2001; Westberry and Siegel, 2006; Bracher et al., 2009; Dupouy et al., 2011), others on size classes (e.g. reviewed in Brewin et al., 2011), and few on multiple plankton functional groups (Alvain et al., 2005, 2008; Raitsoos et al., 2008; Hirata et al., 2011).

In addition to distribution data, data on important plankton traits such as temperature sensitivities or nutrient uptake kinetics have become available for model development (Litchman and Klausmeier, 2008; Buitenhuis et al., 2010; Thomas et al., 2012; Edwards et al., 2012). Thus, there is now ample data for a systematic model evaluation effort. In particular, it is now possible to evaluate not only the bulk properties of marine ecosystem models such as surface chlorophyll *a* against observations and observation-based estimates, but also distributions of individual PFTs and their ecological characteristics.

For DGOMs to be able to resolve and predict changes in ecosystem structure in marine lower trophic level ecosystems and the consequences of such changes for ocean biogeochemistry, models need to be able to reproduce present ecogeography, plankton community structure, as well as the functional diversity required to resolve ecosystem services related to global biogeochemical cycles. Thus, modellers have started to investigate not only questions of marine biogeochemistry, but also questions of marine

BGD

10, 17193–17247, 2013

Distribution, dominance and ecological niches of PFTs

M. Vogt et al.

[Title Page](#)

[Abstract](#)

[Introduction](#)

[Conclusions](#)

[References](#)

[Tables](#)

[Figures](#)

[⏪](#)

[⏩](#)

[◀](#)

[▶](#)

[Back](#)

[Close](#)

[Full Screen / Esc](#)

[Printer-friendly Version](#)

[Interactive Discussion](#)



Helaouët, 2008; Litchman et al., 2007). First, we compare the distribution and dominance patterns of phytoplankton PFTs to patterns derived from satellite estimates. We then identify ecological niches for the dominant phytoplankton PFTs in model and satellite estimates based on environmental conditions such as temperature and nutrient concentrations.

2 Methods

2.1 Model description

In phase 0 of the MAREMIP project, we compare the representation of PFTs in four DGOMs: PlankTOM5 (Buitenhuis et al., 2010), PISCES (Aumont and Bopp, 2006), CCSM-BEC (Moore et al., 2004) and an extended version of NEMURO (Yamanaka et al., 2004; Kishi et al., 2007). We briefly describe the relevant features of each model (Table 1), but refer to the indicated publications for a detailed description of the four different models.

PlankTOM5 represents 3 phytoplankton functional types (pPFTs): silicifiers (diatoms), calcifiers (coccolithophores) and mixed phytoplankton (nanophytoplankton) and 2 zooplankton functional types (zPFTs): micro- and mesozooplankton (Buitenhuis et al., 2010). Phytoplankton growth is limited by iron, dissolved SiO_3 , and a macronutrient (PO_4). The prognostic variables for the 3 pPFTs are their total carbon biomass, iron (Fe), chlorophyll *a*, and silicon content for the silicifiers. For the two size classes of zPFTs, only the biomass is modelled. PlankTOM5 also describes 8 further dissolved and particulate abiotic compartments: dissolved inorganic carbon (DIC), dissolved oxygen and alkalinity (ALK), semi-labile dissolved organic matter (DOM), small (organic) and large (ballasted) sinking particles (POM_s , POM_l), CaCO_3 and particulate SiO_2 . PlankTOM5 is coupled to the NEMO physical model version 2.3 (Madec, 2008) with a resolution of $2^\circ \times 0.5\text{--}2^\circ$ and 31 depth levels, 10 of which are located in the upper 100 m of the water column.

Title Page

Abstract

Introduction

Conclusions

References

Tables

Figures

⏪

⏩

◀

▶

Back

Close

Full Screen / Esc

Printer-friendly Version

Interactive Discussion



Distribution, dominance and ecological niches of PFTs

M. Vogt et al.

Title Page

Abstract

Introduction

Conclusions

References

Tables

Figures

⏪

⏩

◀

▶

Back

Close

Full Screen / Esc

Printer-friendly Version

Interactive Discussion

PISCES represents 2 pPFTs, silicifiers and nanophytoplankton and 2 zPFTs, the micro- and mesozooplankton (Aumont and Bopp, 2006). Calcifiers are implicitly included as a temperature and biomass dependent fraction of nanophytoplankton. Phytoplankton growth is limited by Fe, dissolved SiO_3 , PO_4 , NH_4 and NO_3 . As in PlankTOM5, PISCES simulates the biomass, iron, chlorophyll *a* and silicium content of pPFTs, and the biomass for zPFTs. PISCES comprises 8 further dissolved and abiotic compartments: DIC, dissolved oxygen, ALK, DOM, small and large POM, CaCO_3 and particulate SiO_2 . PISCES is coupled to the NEMO physical model version 3.2 (Madec, 2008) with a resolution of $2^\circ \times 0.5\text{--}2^\circ$ degrees and 31 depth levels.

CCSM-BEC represents 3 pPFTs and 1 generic zPFT (Moore et al., 2004). The pPFTs are silicifiers, small mixed phytoplankton and N_2 fixers (diazotrophs). Calcifiers are implicitly included as a temperature and biomass dependent fraction of nanophytoplankton. The generic zPFT grazes on all size classes of phytoplankton, and its grazing preferences adjust to the prey concentrations. As in PISCES, phytoplankton growth is limited by Fe, SiO_3 , PO_4 , NH_4 and NO_3 , and PFT biomasses and pPFT chlorophyll *a* contents are simulated. CCSM-BEC comprises 7 further dissolved and abiotic compartments: DIC, dissolved oxygen, ALK, DOM and POM, CaCO_3 and particulate SiO_2 . CCSM-BEC is coupled to the Community Climate System Model (CCSM-3), and the ocean component is the 3-D Parallel Ocean Program (POP; Smith and Gent, 2004; Collins et al., 2006). The model resolution is $3.6^\circ \times 0.8\text{--}1.8^\circ$ degrees, and it has 25 depth levels.

NEMURO simulates 2 pPFTs (silicifiers and small mixed phytoplankton) and 3 zPFT: micro-, meso- and macrozooplankton (Kishi et al., 2007). Autotrophic and heterotrophic calcifiers are implicitly included as a constant (10 %) fraction of nanophytoplankton and microzooplankton, respectively. Phytoplankton growth is limited by dissolved Fe, SiO_3 , NH_4 and NO_3 . All PFT carbon biomasses are output variables. The extended version of NEMURO (Yamanaka et al., 2004) comprises 7 further dissolved and abiotic compartments: DIC, dissolved oxygen, alkalinity, DOM and POM, CaCO_3 , and particulate SiO_2 . For MAREMIP phase 0, a simplified iron cycle was implemented in NEMURO.

NEMURO is coupled to the COCO physical model version 3.4 (Hasumi, 2006), which has a resolution of $1^\circ \times 1^\circ$ and 54 depth levels.

All models use the NCEP-NCAR atmosphere reanalysis forcing (Kalnay et al., 1996), but each model uses its own initialization routines. In order to conserve the widest possible spread in simulated ecosystem dynamics, no attempts were made to homogenize model structure, parameterisation, forcing (river inputs and dust), validation or tuning strategies. All equations describing phytoplankton growth and loss processes are given in Hashioka et al. (2012), and a complete list of the parameters corresponding to all pPFTs is given in Appendix A, Table 4. An evaluation of annual mean model nutrients and annual and monthly chlorophyll *a* concentrations relevant to the niche speciation of the different pPFTs considered here is included in Appendix B1 and B2.

2.2 Satellite-derived PFT distributions

We use information from remote sensing on the distribution of phytoplankton from space using two independent algorithms. The PHYSAT algorithm by Alvain et al. (2005) identifies the dominant phytoplankton groups at any given location based on empirical relationships between chlorophyll-normalized water leaving reflectance (nLw) at different wavelengths and phytoplankton diagnostic pigment spectra from High Performance Liquid Chromatography (HPLC; Alvain et al., 2005, 2008, 2012). The algorithm by Hirata et al. (2011) identifies phytoplankton groups, based on empirical relationships between chlorophyll *a* and phytoplankton diagnostic pigment concentrations. Both algorithms have been validated independently with different sets of validation data. Whereas the algorithm by Alvain et al. (2005) is of qualitative nature and indicates the most important pPFT based on differences in relative pigment concentration ranges (dominance), the algorithm by Hirata et al. (2011) quantifies the relative contribution of phytoplankton groups in three size classes to total chlorophyll *a*. Both algorithms were developed for open ocean conditions only.

The pPFTs that can be detected using the PHYSAT method (Alvain et al., 2005) when dominant are the diatoms (silicifiers), the *Synechococcus*-like and

BGD

10, 17193–17247, 2013

Distribution, dominance and ecological niches of PFTs

M. Vogt et al.

Title Page

Abstract

Introduction

Conclusions

References

Tables

Figures

⏪

⏩

◀

▶

Back

Close

Full Screen / Esc

Printer-friendly Version

Interactive Discussion



Distribution, dominance and ecological niches of PFTs

M. Vogt et al.

Title Page

Abstract

Introduction

Conclusions

References

Tables

Figures

⏪

⏩

◀

▶

Back

Close

Full Screen / Esc

Printer-friendly Version

Interactive Discussion

Prochlorococcus-like picophytoplankton, eukaryotic nanoflagellates (mixed phytoplankton) and the two haptophyte plankton taxa of coccolithophores (calcifiers) and *Phaeocystis* (DMS producers), although coccolithophore dominance is known to be underestimated by the PHYSAT (and all other radiance-based) method(s), due to fixed thresholds in the SeaWiFS algorithm (Alvain et al., 2008). The PHYSAT method has been evaluated using in situ measurements in Alvain et al. (2008, 2012), and good agreement has been found for nanoflagellates (82 % of correct identifications of dominance). The method is also reliable for diatoms (73 % of correct identification), but it is less reliable for the detection of the two picophytoplankton classes, where 57 % of *Synechococcus* and 61 % of *Prochlorococcus*-dominated waters samples were correctly identified. However, for the two picophytoplankton groups, errors are mainly due to a misattribution of the signal of one group to the other, since both groups are similar both in signal and regional distribution (Alvain et al., 2008).

The method of Hirata et al. (2011) quantifies the relative contribution of seven pPFTs in three size classes to total chlorophyll *a*: diatoms, dinoflagellates, green algae, prymnesiophytes, pico-eukaryotes, pico-prokaryotes, and *Prochlorococcus sp.* The root mean squared error (RMSE) in percent associated with the relative contribution to total chlorophyll *a* varies depending on the pPFT, with 8.0 % for diatoms, 8.3 % for microphytoplankton, 8.6 % for nanophytoplankton, and 7.1 % for picophytoplankton, with an average of 6.0 % for all pPFTs. Here, we apply the formula given in Hirata et al. (2011) to gridded monthly mean SeaWiFS chlorophyll *a*. Note that the uncertainty in chlorophyll *a* adds an additional error component to these estimates.

2.3 Association between satellite and model PFTs

For the investigation of ecological niches, the different plankton groups detected by the satellite have been grouped into pPFTs according to the classification of Le Quéré et al. (2005), and compared with the respective model pPFTs. Satellite-derived pPFTs comprise the silicifiers (diatoms), calcifiers (coccolithophores or prymnesiophytes), DMS producers (*Phaeocystis*), and the nano- (nanoflagellates or green algae) and pico-

**Distribution,
dominance and
ecological niches of
PFTs**

M. Vogt et al.

[Title Page](#)[Abstract](#)[Introduction](#)[Conclusions](#)[References](#)[Tables](#)[Figures](#)[⏪](#)[⏩](#)[◀](#)[▶](#)[Back](#)[Close](#)[Full Screen / Esc](#)[Printer-friendly Version](#)[Interactive Discussion](#)

phytoplankton (*Prochlorococcus* and *Synechococcus*, or *Prochlorococcus*, picoeukaryotes, total picoprokaryotes, respectively). Thus, satellite diatoms have been associated with model silicifiers, and the contributions by all small nano- and picophytoplankton groups have been added up, and compared with modelled nanophytoplankton. For the niche calculations, a distinction between satellite-derived nano- and picophytoplankton has been made.

Calcifiers (coccolithophores) have a satellite analogue in Alvain et al. (2005), although coccolithophore dominance is known to be underestimated by reflectance-based methods (Alvain et al., 2008). Coccolithophores contain the diagnostic pigment markers hexanoyloxyfucoxanthin (Hex) and butanoyloxyfucoxanthin (But), and are thus included in the prymnesiophyte class determined by Hirata et al. (2011). Thus, the satellite-derived prymnesiophyte niche (P) is assumed to contain the coccolithophore niche (C ; in mathematical terms: $P \subset C$, but $P \neq C$). Other satellite estimates to detect coccolithophore blooms exist (e.g. Balch et al., 1996; Brown and Yoder, 1994; Iglesias-Rodríguez et al., 2002; Smyth et al., 2004; Shutler et al., 2013), but these estimates have not been included in the current analysis due to their focus on a single PFT, and on bloom conditions only.

Nitrogen fixers (diazotrophs), are modelled to represent *Trichodesmium* in CCSM-BEC. *Trichodesmium* is a filamentous, bloom-forming cyanobacteria, which has no satellite-analogue in Alvain et al. (2005), and thus cannot be compared directly with this satellite estimate. However, *Trichodesmium* contains the diagnostic pigment zeaxanthin, on which the empirical pico-prokaryote formulation by Hirata et al. (2011) is based. Thus, as in the case of the calcifiers, the HPLC pigment-derived pico-prokaryote niche by Hirata et al. (2011) is assumed to contain the *Trichodesmium* niche. Other satellite estimates to detect *Trichodesmium* exist (e.g. Subramaniam and Brown, 2001; Westberry and Siegel, 2006; Bracher et al., 2009; Dupouy et al., 2011), but these estimates have not been included in the current analysis due to their focus on a single PFT, and on bloom conditions only.

2.4 Biogeochemical and environmental data

For model validation and the niche calculations, we use surface nitrate (NO_3) and silicate (SiO_3) measurements from World Ocean Atlas (Garcia et al., 2005) and gridded iron measurements from Aumont et al. (2006). We use sea surface temperature (SST) from the World Ocean Atlas (2005), and mixed layer depth (MLD) from de Boyer Montégut et al. (2004). Furthermore, we use monthly mean surface chlorophyll *a* from SeaWiFS on a $1^\circ \times 1^\circ$ grid.

2.5 Data treatment

Modelled monthly mean surface data for the years 1996–2007 were projected from the original model grids of each model onto a regular $360^\circ \times 180^\circ$ grid, in order to match the World Ocean Atlas grid. While models have been forced with interannually varying fields, we focus our analysis on annual and monthly climatologies here. SeaWiFS chlorophyll *a* and model data for the period 1996–2007 was averaged, and the monthly averaged climatologies were used.

2.6 Definition of dominance and coexistence

Dominance patterns of the individual pPFTs have been calculated as a function of pPFT biomass on a monthly and annual basis, where dominance was attributed to the pPFT constituting more than 50 % of the biomass at any given location and during any given month or year. For Hirata et al. (2011), dominance was defined based on the fraction of total chlorophyll *a* derived from the empirical relationships being larger than 0.5. Since dominance in Alvain et al. (2005) is based on ranges and thresholds of relative pigment concentrations and the corresponding nLw signal at different wavelengths, no absolute biomass fraction corresponding to this definition of dominance can be indicated. Coexistence was defined as a state in which several pPFTs contribute to

BGD

10, 17193–17247, 2013

**Distribution,
dominance and
ecological niches of
PFTs**

M. Vogt et al.

Title Page

Abstract

Introduction

Conclusions

References

Tables

Figures

⏪

⏩

◀

▶

Back

Close

Full Screen / Esc

Printer-friendly Version

Interactive Discussion



total biomass simultaneously, but no single group contributed more than 50 % to total biomass.

Dominance was chosen as a metric for model inter-comparison, since this allowed the inter-comparison of models with both satellite estimates simultaneously. Furthermore, in most models, PFTs are numerically prevented from going extinct, and low concentrations of all pPFTs are present at all times. While this may be the case also in natural marine ecosystems (Baas Becking, 1934), we found that the relative biomass proportions of different PFTs are still highly uncertain in models, whereas dominance patterns are more consistently modelled (see e.g. Sect. 3.1 below).

2.7 Definition of niche space

The full range of environmental conditions under which an organism prospers describes its fundamental ecological niche (Hutchinson, 1957). The so-called realized ecological niche is smaller than the fundamental niche, and is a result of pressure from, and interactions with, other organisms in the marine environment. Here, we assess a proxy of realized ecological niche space, based on dominance patterns of the different pPFTs under different environmental conditions. Ecological niche space was defined as the hypervolume spanned by independent factors limiting phytoplankton growth. We chose surface NO_3 concentration, MLD and SST to be the axes of a 3-dimensional niche (sub-)space, because models parameterize pPFT growth as

$$\mu(x, y, z, t)^{P_i} = \mu_{\max}^{P_i} L_{\text{nut}} f(T) f(I) \quad (1)$$

where μ is the current specific growth rate (1/d) of any given pPFT P_i at a certain location (x, y, z, t) , and it is a product of the maximal growth rate μ_{\max} , a nutrient limitation term L_{nut} , which is often parameterized as the minimum of several Michaelis–Menten functions (Michaelis and Menten, 1913), a temperature term $f(T)$, often in the form of a Q_{10} function (Eppley, 1972) and a light harvesting function $f(I)$ which contains a parameterisation of carbon uptake during photosynthesis (e.g. Geider et al.,

BGD

10, 17193–17247, 2013

Distribution, dominance and ecological niches of PFTs

M. Vogt et al.

Title Page

Abstract

Introduction

Conclusions

References

Tables

Figures

⏪

⏩

◀

▶

Back

Close

Full Screen / Esc

Printer-friendly Version

Interactive Discussion



1998). Annual mean MLD serves as a proxy for the solar radiation dose received by the different pPFTs, despite the fact that variations in MLD also correlate with variations in nutrient, temperature, chlorophyll and biomass conditions. Because we only study the surface distribution of pPFTs, we use SST to calculate the temperature niche. We base our niche calculation on global concentrations of NO_3 . Niches based on surface PO_4 and SiO_3 have also been investigated, but the strong collinearity between these macronutrients leads to similar patterns to those based on NO_3 (data not shown). Iron has been shown to be important for phytoplankton distribution patterns in HNLC regions (Martin, 1990; Martin et al., 1994), but due to the limited availability of observed iron concentration data for comparison with the model fields (Tagliabue et al., 2012; Dutkiewicz et al., 2012) we limit the niche analysis to macronutrient availability. In this initial analysis, we neglect loss processes such as grazing by zooplankton and differences in mortality, which could also affect seasonal succession patterns and niche characteristics (Hashioka et al., 2012).

2.8 Niche characterisation using a general additive model

We use Generalized Additive Models (GAMs; Weber, 2006) to characterise the realized niches of each pPFT within both the DGOMs and the satellite observations, and to extract broad-scale patterns. GAMs are a statistical modelling technique that describe a response variable as an additive linear function of several predictor variables. However, unlike traditional “straight-line” regression approaches, GAMs can represent the response using non-parametric spline smoothing functions. Furthermore, the response is not limited to the assumption of a Gaussian error structure, as in more traditional approaches: Binomial, Poisson, Negative Binomial and, in this case, Bernoulli observation models, amongst others, can also be considered.

Here we apply GAMs as a data exploration and simplification technique to explore niche-space and characterise the probability of an individual pPFT in a given DGOM/satellite being dominant under a specified set of environmental conditions. As mentioned above, dominance at pixel i , D_i , was defined as a pPFT constituting more

Distribution, dominance and ecological niches of PFTs

M. Vogt et al.

Title Page

Abstract

Introduction

Conclusions

References

Tables

Figures



Back

Close

Full Screen / Esc

Printer-friendly Version

Interactive Discussion



than 50 % of total annual mean biomass for each pixel. The observed dominance was then modelled as follows:

$$D_i \sim \text{Bernoulli}(\pi_i) \quad (2)$$

$$\text{logit}(\pi_i) = \text{te}(\text{NO}_{3j}, \text{SST}_j, \text{MLD}_j) \quad (3)$$

where D_i is the dominance of the pPFT in question (coded as 1/0), NO_{3j} , SST_j , and MLD_j are surface NO_3 , SST, and MLD, respectively at pixel i , and π_i is the modelled probability of the pPFT being dominant. A logit function is used to map (“link”) the linear predictor, a three-dimensional tensor-product spline-smoother with a cubic basis function, $\text{te}(\dots)$ (Wood 2006) and a domain on the real number line i.e. $[-\infty, \infty]$, to the modelled probability π_i (domain $[0, 1]$). The dominance “observations” are assumed to exhibit a Bernoulli distribution about the expected probability π_i .

The quality of the GAM fit, and thereby its ability to characterise the niche, was quantified based on the “explained deviance” statistic: this statistic can be best understood as an analog of the coefficient of determination (R^2) in linear-regression, which is often interpreted as the proportion of variance explained.

GAM models were fitted for each pPFT within each DGOM/satellite data set. In cases where there were more than two pPFTs, cohabitation at similar biomass levels (i.e. no group more than 50 %) was also added as a possible outcome, and therefore a GAM was fitted accordingly to determine the probability of this occurrence. The fitted GAMs for each outcome were then evaluated in niche space and the most likely dominant group determined. Finally, the fitted dominance probabilities were mapped back into geographical space to allow visual comparisons.

BGD

10, 17193–17247, 2013

Distribution, dominance and ecological niches of PFTs

M. Vogt et al.

[Title Page](#)

[Abstract](#)

[Introduction](#)

[Conclusions](#)

[References](#)

[Tables](#)

[Figures](#)

[⏪](#)

[⏩](#)

[◀](#)

[▶](#)

[Back](#)

[Close](#)

[Full Screen / Esc](#)

[Printer-friendly Version](#)

[Interactive Discussion](#)

is not possible, since they do not quantify this group explicitly. In the low latitudes, satellite-based estimates of biomass are dominated by the pico- and nanophytoplankton size class (Fig. 1e), with a high fraction of green algae and pico-prokaryotes, which constitute a fairly constant fraction of biomass at all latitudes (not shown). The closest satellite equivalent to the coccolithophores, the prymnesiophytes, contributes less than 12 % to total satellite-derived carbon in the temperate latitudes of the Northern Hemisphere (NH). Compared to Hirata et al. (2011), models tend to overestimate the relative contribution of diatoms to annual mean surface biomass (Fig. 1e).

3.2 Annual mean dominance patterns

Figure 2 shows the simulated dominance patterns for annual mean biomass of the four models, as compared to the chlorophyll-based annual mean dominance patterns detected by Alvain et al. (2005) and Hirata et al. (2011). All models simulate diatom dominance in the high latitudes, and mixed phytoplankton dominance in the temperate and low latitudes. However, models appear to overestimate the area of annual mean diatom dominance, both in the Southern Ocean and in the Arctic when compared to the two satellite estimates.

Coccolithophores in PlankTOM5 dominate at locations where pico- and nanophytoplankton dominance is detected by the satellites. In both satellite estimates, coccolithophore dominance is rare on the annual mean. The Hirata et al. (2011) algorithm predicts large areas in the NH where none of the individual pPFTs constitutes more than 50 % of total biomass (Fig. 2e; areas designated by “coex”). Areas of coexistence in PlankTOM5 agree with those of Hirata et al. (2011), but coexistence is less wide spread in the model, also due to the comparatively low number of pPFTs included in these models. Diazotrophs do not dominate the annual mean biomass in CCSM-BEC. However, they constitute a small fraction of biomass in the Tropics and Subtropics. Table 3 summarises the fraction of grid cells where a pPFT is dominant on an annual mean in both numerical and satellite models.

[Title Page](#)

[Abstract](#)

[Introduction](#)

[Conclusions](#)

[References](#)

[Tables](#)

[Figures](#)

[⏪](#)

[⏩](#)

[◀](#)

[▶](#)

[Back](#)

[Close](#)

[Full Screen / Esc](#)

[Printer-friendly Version](#)

[Interactive Discussion](#)



3.3 Monthly dominance patterns

Annual mean dominance patterns are most revealing in regions that have a low seasonality and good coverage. Neither is the case for high latitude regions: biomass increases exponentially in phytoplankton blooms during the short summer months when light conditions permit growth, and satellites do not observe the high latitudes during the winter months. We show here the dominance patterns for four selected months (December, March, June and September), to get a better understanding of seasonal ecosystem dynamics in the bloom regions (Fig. 3). A seasonal cycle is clearly visible in the observations and, to a lesser degree, in the models.

In December, all models show a high abundance of diatom dominated grid cells in the Southern Ocean, consistent with observations. In the NH, all models except for PISCES predict diatoms to dominate total biomass in the Arctic Ocean and parts of the temperate latitudes, where total biomass is low during this month. Since the satellites do not detect phytoplankton patterns in the high latitudes of the NH during those months due to the low light conditions, we cannot validate model simulations in those areas.

In March, diatom dominated areas in the Southern Ocean decrease in all models except for PlankTOM5, where diatom dominance spreads. Models simulated an increase of diatom dominated areas in the NH, where both satellite methods predominantly detect nanophytoplankton dominance. Coccolithophore dominance in PlankTOM5 is highest in March, but the boundaries of coccolithophore dominated areas do not shift significantly over the year. Coccolithophores in PlankTOM5 tend to inhabit niches where satellite estimates detect pico- (Alvain et al., 2005) or pico- and nanophytoplankton dominance (Hirata et al., 2011). Thus, simulated coccolithophores tend to inhabit niches that are dominated by plankton types of a similar or smaller size class in satellite estimates.

In June, diatom dominated areas in the NH are shrinking in some models (NEMURO, CCSM-BEC), but still expanding in others (PlankTOM5, PISCES). This indicates that

BGD

10, 17193–17247, 2013

Distribution, dominance and ecological niches of PFTs

M. Vogt et al.

Title Page

Abstract

Introduction

Conclusions

References

Tables

Figures

⏪

⏩

◀

▶

Back

Close

Full Screen / Esc

Printer-friendly Version

Interactive Discussion



Distribution, dominance and ecological niches of PFTs

M. Vogt et al.

[Title Page](#)

[Abstract](#)

[Introduction](#)

[Conclusions](#)

[References](#)

[Tables](#)

[Figures](#)

[⏪](#)

[⏩](#)

[◀](#)

[▶](#)

[Back](#)

[Close](#)

[Full Screen / Esc](#)

[Printer-friendly Version](#)

[Interactive Discussion](#)

models differ in the simulation of phytoplankton succession during the spring bloom, both in terms of the relative biomass fraction attributed to this group, and also in terms of the timing of the spring bloom (see e.g. Hashioka et al., 2012). The large areas of diatom dominance in the Southern Hemisphere (SH) in CCSM-BEC and NEMURO occur at very low biomasses, as these models predict diatoms to constitute a large fraction of biomass also in the SH winter, which contributes to the SH biomass pattern in Fig. 1.

In September, all models show areas with diatom dominance in the Arctic, and several models predict increased areas of diatom dominance along the coasts and in upwelling areas of the SH. Satellite estimates detect small areas of diatom dominance in the North Pacific and the Southern Ocean and the continental coasts. However, neither the method of Alvain et al. (2008) nor the one by Hirata et al. (2011) was constructed for a correct identification of phytoplankton pattern in coastal and upwelling areas with high chlorophyll *a* concentrations.

Diazotrophs in CCSM-BEC do not dominate total biomass during any given month, and are thus not represented in Fig. 3. As in Fig. 2, the algorithm by Hirata et al. (2011) identifies extended regions where none of the detected pPFTs constitutes more than 50 % of biomass. In June and September, large areas of the NH are not dominated by any single pPFT (Fig. 3). While the cohabitation of more than 2 pPFTs with equally high contributions to biomass is possible both in PlankTOM5 and in CCSM-BEC, these models rarely simulate an equal biomass distribution among pPFTs (Fig. 3).

3.4 Ecological niches of the dominant pPFTs: NO₃, SST and MLD

We use the GAM described above (Sect. 2.8) to characterise the dominance niches for each model and pPFT as a function of NO₃ concentration and SST (Fig. 4). The GAM explained the majority of the variability (deviance) in the simulated dominance patterns (typically around 65–70 % on average) for the models, but it performs less well for the two satellite estimates (around 40 % of deviance explained on average). Exploratory analyses (Appendix C) suggested that although the effect of MLD was

statistically significant, the “added-value” (in terms of addition explained deviance) of included MLD in the GAM model was relatively minor for the four models (5–10 % gain in explained deviance; Fig. 7), possibly also because MLD is highly correlated with SST and NO₃. In order to simplify visualisation and interpretation, the remainder of this analysis is therefore performed with the two variables, SST and NO₃, that explain the largest proportion of the deviance.

There are several general patterns that are consistent between models. For all models, the GAM predicts diatom dominance at low temperatures and high NO₃ concentrations (Fig. 4a–d). Models simulate diatom dominance for a wider range of environmental conditions (Fig. 2), but the simulated diatom niches are constrained to a tight range of environmental conditions for the two satellites. For diatom dominance, the statistically modelled probability based on annual mean NO₃ concentration and SST explains the majority of the variance (65.2–66.6 % of deviance explained). For the satellite estimates, the deviance explained is much lower (44.6 % and 32.7 % for Alvain et al., 2008 and Hirata et al., 2011, respectively). On annual time scales, modelled diatom dominance is correlated more strongly with annual mean environmental conditions than satellite-derived diatom dominance.

Consistent with expectations for nanophytoplankton, the GAM predicts its dominance over a wide range of temperatures and nutrient concentrations for all models (Fig. 4). In addition, satellites resolve the distinction between nano- and picophytoplankton, two size classes that are not distinguished in the models. Coexistence, defined as the area in niche space where none of the pPFTs comprises more than 50 % of biomass, rather than dominance is wide-spread in Hirata et al. (2011), cannot be detected in Alvain et al. (2005) nor simulated in PISCES and NEMURO, and is rare in PlankTOM5 and, by model construction, in CCSM-BEC (low total diazotroph biomass; see Fig. 2).

For PlankTOM5, the GAM predicts a narrow niche for diatom dominance at low temperatures and high nutrient concentrations (Fig. 4a). The diatom niche is divided into two sub-clusters, each describing one hemisphere. PlankTOM5 simulates an extended region in niche space to be dominated by coccolithophores, (Fig. 2, Fig. 4), but prym-

BGD

10, 17193–17247, 2013

Distribution, dominance and ecological niches of PFTs

M. Vogt et al.

[Title Page](#)

[Abstract](#)

[Introduction](#)

[Conclusions](#)

[References](#)

[Tables](#)

[Figures](#)

[⏪](#)

[⏩](#)

[◀](#)

[▶](#)

[Back](#)

[Close](#)

[Full Screen / Esc](#)

[Printer-friendly Version](#)

[Interactive Discussion](#)



nesiophyte dominance on the annual mean is rare according to the two satellites. In PlankTOM5, coccolithophores tend to inhabit niches that are characteristic of picophytoplankton (*Prochlorococcus* and *Synechococcus*-like phytoplankton, Fig. 2) in the satellite estimates.

PISCES shows a considerable fraction of pixels dominated by diatoms on the annual mean, both for the NH and the SH (Fig. 2). In niche space, the GAM predicts diatoms to populate a wide range of low-intermediate nutrient concentrations, and low-intermediate temperatures. PISCES is the only model where diatoms are consistently dominant in most upwelling regions (Agulhas, Western Boundary Current Systems), which is explained by the sub-niche of diatoms at intermediate-high nutrient concentrations.

CCSM-BEC simulates a large area of diatom dominance in the Southern Ocean and the Arctic Ocean (Fig. 2). Both diatom and nanophytoplankton dominate niches are characterised by a wide range of nutrient concentrations and temperatures, but diatoms dominate at lower temperatures and higher nutrient concentrations. Diazotrophs never dominate on the annual mean, but occur at high temperatures ($> 20^{\circ}\text{C}$), and at intermediate nutrient concentrations. A comparison with Fig. 1 shows, that the niche representation of this pPFT is fairly consistent with the niches of satellite-derived picophytoplankton.

For NEMURO's ecosystem, the GAM derives two distinct niches for the dominance of diatoms and nanophytoplankton (Fig. 4c). Diatoms dominate the entire Southern Ocean ecosystem, and are abundantly dominant in the Arctic and temperate NH Oceans (Fig. 2). They can dominate over a wide range of temperatures and at intermediate-high NO_3 concentrations. As in the other models, nanophytoplankton dominate in regions with low nutrient concentrations and intermediate-high temperatures.

Since the deviance explained by the GAM is relatively low for the satellites (Appendix C, Fig. 7), other factors than those investigated here control a significant fraction of the variability in the dominance patterns. However, for both satellites, diatoms

BGD

10, 17193–17247, 2013

**Distribution,
dominance and
ecological niches of
PFTs**

M. Vogt et al.

Title Page

Abstract

Introduction

Conclusions

References

Tables

Figures

⏪

⏩

◀

▶

Back

Close

Full Screen / Esc

Printer-friendly Version

Interactive Discussion



dominate at low to intermediate temperatures, but at variable and differing nutrient concentrations (Fig. 4e and f). In Alvain et al. (2008), diatoms dominate niche space where nutrient concentrations are high ($[\text{NO}_3] > 10 \text{ mmol m}^{-3}$), and annual mean temperatures are low ($\text{SST} < 0^\circ\text{C}$), i.e. close to the Antarctic continent (Fig. 4e). In Hirata et al. (2011), diatoms inhabit their largest niche at low nutrient concentrations and low to intermediate SSTs (Fig. 2). This niche is located in the North Pacific, where Alvain et al. (2005) detect nanophytoplankton dominance.

In both satellite algorithms, nanophytoplankton occupy a large area in niche space, and they are found at a wide range of MLDs, SSTs and NO_3 concentrations. Furthermore, picophytoplankton dominate at high SSTs and low nutrient concentrations. Whereas picophytoplankton dominance is separated from nanophytoplankton dominance by differences in SST only in Alvain et al. (2005), picophytoplankton dominance is confined to a low NO_3 and high SST niche in Hirata et al. (2011). Coccolithophore/Haptophyte dominance detected by the satellites is rare, which is why the GAM does not model a sizeable niche for this group.

3.5 Spatial probability patterns for the dominance of diatoms

We now apply the GAM to determine the probability of pPFT dominance on the global scale. Here, we only show the probability of diatom dominance for both model and satellite estimates, since models and satellite differ most in the representation of this group (Fig. 5). Models predict a high probability of diatom dominance in the high latitudes, and a low probability in the low latitudes. Satellite estimates predict a low probability for dominance of diatoms on the annual mean almost everywhere. The results of the statistical model are consistent with our findings in Figs. 2 and 3. In the annual mean, models and satellite estimates do not agree on the extent of diatom dominance in the high latitudes of both hemispheres.

BGD

10, 17193–17247, 2013

Distribution, dominance and ecological niches of PFTs

M. Vogt et al.

Title Page

Abstract

Introduction

Conclusions

References

Tables

Figures

⏪

⏩

◀

▶

Back

Close

Full Screen / Esc

Printer-friendly Version

Interactive Discussion

4 Discussion

Current Dynamic Green Ocean Models simulate 2–3 pPFTs, and all have at least two common size classes: large diatoms and a group of small mixed phytoplankton. In contrast to models, satellite pPFTs divide the small size class into nano- and picophytoplankton, and a varying number of subgroups. Given that neither nanophytoplankton nor picophytoplankton have been associated with a specific biogeochemical function except for their contribution to background NPP and export (Le Quéré et al., 2005) and that their N : P ratios are often fixed to the Redfield ratio, the DGOMs analysed here are left with only one common pPFT that acts differentially on the elemental cycles of several nutrients and other chemical compounds: the silicifiers (diatoms), which use silicate and contribute significantly to high latitude productivity and export (Buesseler, 1998; Goldman, 1993). Recent model studies suggest that the differential uptake of NO_3 and PO_4 , as well as between pPFT differences in cellular N : P ratios are crucial for our understanding of the nitrogen cycle (Weber and Deutsch, 2010, 2012). Therefore, either a more flexible plankton stoichiometry or a sub-division of the small phytoplankton group into calcifiers, nitrogen fixers, DMS producers etc. would be desirable (Le Quéré et al., 2005). However, two of the models studied here already include an explicit representation of calcifiers or nitrogen fixers, and all models contain an implicit representation of calcifiers as a fraction of nanophytoplankton, thus advancing model development in this regard.

4.1 Biomass distribution and dominance patterns

A critical look at the annual and monthly mean dominance patterns and the global and zonal mean surface biomass estimates presented in Sect. 3.1 suggests that the discrepancy between simulated and satellite-based relative extent of diatom and non-diatom dominated areas for the global ocean may raise important questions (Figs. 2 and 3). In the satellite estimates, pPFTs pertaining to the small phytoplankton size class appear to dominate most ocean regions (Figs. 2–4), yet diatom dominance is

BGD

10, 17193–17247, 2013

Distribution, dominance and ecological niches of PFTs

M. Vogt et al.

Title Page

Abstract

Introduction

Conclusions

References

Tables

Figures

⏪

⏩

◀

▶

Back

Close

Full Screen / Esc

Printer-friendly Version

Interactive Discussion



be underestimated since empirical relationships were applied to monthly and annual mean chlorophyll *a*. Spatial averaging into 1° bins may also lead to an underestimation of patchy diatom distributions.

Alternatively, diatoms could dominate at deeper depths than the penetration depth of the satellites (Gordon and McCluney, 1975). The model-data misfit could thus be due to models consistently simulating diatom dominance in too shallow waters. However, preliminary results from Peloquin et al. (2013) suggest that fucoxanthin concentrations, indicative of diatom presence, are highest in the upper 30 m of the water column at almost all latitudes. This is confirmed by in situ observations of diatom biomass (Leblanc et al., 2012). Thus, errors in simulated vertical ecosystem structure are unlikely to explain the differences between models and satellites.

Last but not least, diatoms could produce the majority of export despite the fact that their annual mean biomass is smaller than expected. This is supported by some observational evidence that find that diatoms dominate export also in regions where other plankton groups are quantitatively more important (e.g. Nelson and Brzezinski, 1997). It is conceivable that important biogeochemical processes are predominantly carried out by rare species and not by the groups that dominate an ecosystem at any given time, but at present few DGOMs allow for the quantification of such effects. A quantitative investigation of the relative biomass fractions of all PFTs and their link to patterns of biogeochemically relevant ecosystem functions based on observational data would be desirable, but co-located data is still limited on the global scale (Buitenhuis et al., 2013b).

Other important biogeochemical functions, such as DMS production or calcification, seem to be carried out by pPFTs that the satellite models detect to be groups that are either rare in terms of the extension of spatial dominance, or dominant only during short times (*Phaeocystis*, coccolithophores). If satellite estimates are reliable, a better representation of bloom dynamics and phytoplankton succession may be necessary in order to resolve the level of complexity required to represent all processes important for ocean biogeochemistry. The timing and magnitude of the bloom, relative abundance

**Distribution,
dominance and
ecological niches of
PFTs**

M. Vogt et al.

[Title Page](#)[Abstract](#)[Introduction](#)[Conclusions](#)[References](#)[Tables](#)[Figures](#)[Back](#)[Close](#)[Full Screen / Esc](#)[Printer-friendly Version](#)[Interactive Discussion](#)

**Distribution,
dominance and
ecological niches of
PFTs**

M. Vogt et al.

[Title Page](#)[Abstract](#)[Introduction](#)[Conclusions](#)[References](#)[Tables](#)[Figures](#)[Back](#)[Close](#)[Full Screen / Esc](#)[Printer-friendly Version](#)[Interactive Discussion](#)

of diatoms and nanophytoplankton at the bloom maximum, and the relation between top-down and bottom-up processes has recently been discussed in detail in Hashioka et al. (2012) for the same set of MAREMIP phase 0 models. Diatoms have been found to be important contributors to biomass at the bloom maximum, with a contribution of > 70 % to total biomass in three out of the four models. However, mechanisms that controlled diatom dominance during the bloom differed widely among models. In particular, the relative importance between top-down (grazer-mediated) and bottom-up processes were widely different between models. In order to better understand phytoplankton dynamics and competition during blooms, the quantification of biogeochemical function and species interactions on temporal scales shorter than one month is necessary. In addition, it is crucial to constrain the controls of the higher tropic levels with experimental data (Sailley et al., 2013).

4.2 Modelled ecological niches of phytoplankton PFTs

Models clearly simulate different ecological niches for the dominance of the different pPFTs that they represent. In particular, the diatom niche tends to be separated from the niche of the smaller-sized phytoplankton by lower temperature values and higher nutrient concentrations. In contrast to the satellite estimates, diatoms in models are found to be dominant on the annual mean at a wide range of MLDs. This is mostly due to the fact that models simulate diatom dominance in more months of the year than satellites (Bopp et al., 2005). In combination with the findings of Hashioka et al. (2012), the patterns in Figs. 4 and 5 suggest that the mismatch between model and satellite estimates of the diatom niche may be due to a poor representation of bloom dynamics and phytoplankton succession in the models: while models tend to simulate a variable but significant fraction of diatoms during the bloom maximum consistent with observation, diatoms tend to stay important throughout the year rather than being succeeded by other pPFTs (Bopp et al., 2005). This suggests that the representation of phytoplankton phenology needs to be improved in the models.

observed biomass and distribution patterns for this taxon will shed more light on the factors controlling the position and extent of their ecological niche (Luo et al., 2013, Brun et al., 2013).

4.3 Caveats of this study

This study attempts to quantitatively and qualitatively compare ecological properties of the four DGOMs participating in MAREMIP phase 0 beyond the evaluation of chlorophyll *a* patterns only. Such studies still suffer from the fact that in parallel to the increase of independent sources of validation data such as the pPFT distribution from space used here (Alvain et al., 2005; Hirata et al., 2011), suitable metrics to quantify model-data fit for ecological properties still need to be developed. Thus, there are several caveats that need to be borne in mind when interpreting our results:

Firstly, in this initial study, we use annual and monthly mean environmental conditions to characterize the distribution and dominance patterns of the modelled phytoplankton community, aggregated onto a coarse $1^\circ \times 1^\circ$ grid. While such an aggregation will capture north–south gradients and large scale patterns, we are unable to characterize interannual variability, seasonal succession patterns, bloom events or areas with large spatial heterogeneity. However, the temporal averaging of highly variable biological data onto longer time intervals has been shown to decrease the accuracy of the satellite estimates (Alvain et al., 2008). Thus, an investigation of daily and weekly time scales would lead to a better quantification of the respective phytoplankton niches. Similarly, phytoplankton composition has been shown to vary significantly on interannual to decadal time scales due to changes in climate (e.g. Alvain et al., 2013) or during ENSO cycles (e.g. Alvain et al., 2008; Masotti et al., 2011). Hence, the study of interannual variability in dominance patterns might lead to a more robust identification of the drivers of phytoplankton biogeography. However, for the latter applications, high resolution global scale co-located nutrient, light and temperature data would be required. Similar arguments holds for the aggregation of data onto a coarse spatial grid.

Distribution, dominance and ecological niches of PFTs

M. Vogt et al.

[Title Page](#)

[Abstract](#)

[Introduction](#)

[Conclusions](#)

[References](#)

[Tables](#)

[Figures](#)

[⏪](#)

[⏩](#)

[◀](#)

[▶](#)

[Back](#)

[Close](#)

[Full Screen / Esc](#)

[Printer-friendly Version](#)

[Interactive Discussion](#)



2007; Bruggeman and Kooijman, 2007). In order to simulate realistic plankton communities, we must exploit the wealth of new data that is available (Buitenhuis et al., 2013b; Thomas et al., 2012; Edwards et al., 2012; Barton et al., 2013), and incorporate findings from theoretical ecology to widen our ecological understanding of food web dynamics (Sailley et al., 2013) and ecosystem functioning. Only then will our models be able to quantify the impacts of future changes for marine ecosystems, and their response to climate change.

Appendix A

Model parameters

All model parameters describing phytoplankton growth in PlankTOM5, PISCES, CCSM-BEC and NEMURO are given in Table 4 below.

Appendix B

Model validation

B1 Physical variables and nutrient concentrations

All models simulate annual mean surface PO_4 and NO_3 concentrations with Pearson correlation coefficients (ρ) > 0.9 and standard deviations (σ_D) close to the observational value (0.72 mmol L^{-1} and 7.62 mmol L^{-1} , respectively). The RMSE is low (ca. $\frac{1}{3}$ of the mean). Correlation coefficients for simulated annual surface SiO_3 are lower ($\rho = 0.74\text{--}0.92$), with only NEMURO and CCSM showing $\rho > 0.9$. In addition, the standard deviations in SiO_3 concentrations tend to be over- (PISCES, CCSM-BEC and NEMURO; range: $\sigma = 22.24\text{--}28.68 \text{ mmol L}^{-1}$) or underestimated (PlankTOM5,

BGD

10, 17193–17247, 2013

**Distribution,
dominance and
ecological niches of
PFTs**

M. Vogt et al.

Title Page

Abstract

Introduction

Conclusions

References

Tables

Figures

⏪

⏩

◀

▶

Back

Close

Full Screen / Esc

Printer-friendly Version

Interactive Discussion

$\sigma = 13.16 \text{ mmol L}^{-1}$) by the models. The model data agreement is poorest for annual mean surface iron concentrations: None of the models can explain more than 40 % of the spatial variability ($0.20 > \rho > 0.4$). For iron, simulated σ are under- or overestimated by a factor of 2 or higher ($\sigma_{\text{obs}} = 0.43 \text{ nM}$). RMSEs are 1–3× the average concentrations. All in all, models provide a consistent picture of oceanic macronutrients such as NO_3 and PO_4 , but deviations from the observations are larger for SiO_2 and trace elements such as iron. For SST, all models obtain a $\rho > 0.995$ and a σ close to the observational value of 10.46°C . The RMSE is below 1°C . Modelled MLDs are less consistent with observations: Correlation coefficients ρ are lower than $\rho = 0.7$, and most models underestimate σ . The average RMSE is of the order of the annual mean MLD.

B2 Chlorophyll a: comparison with SeaWiFS satellite data

Figure 6 shows the global patterns of annual mean surface chlorophyll *a* for PlankTOM5, PISCES, NEMURO, and CCSM-BEC, as compared to chlorophyll *a* from the SeaWiFS satellite for the years 1997–2006. All models correctly simulate the gradient in chlorophyll between the high and the low latitudes, and show the lowest chlorophyll *a* concentrations in the subtropical gyres. Highest chlorophyll *a* concentrations are simulated close to the coasts, and in the North Atlantic and North Pacific, as well as in the Southern Ocean and close to the Antarctic continent, in agreement with observations. NEMURO shows highest chlorophyll- *a* concentrations in the Southern Ocean, which is due to a simplified iron limitation in this model. PlankTOM5 and CCSM-BEC underestimate chlorophyll *a* concentrations in the North Atlantic. The accurate simulation of absolute annual mean chlorophyll *a* concentrations, however, is still challenging for models. Pixel-wise correlations between SeaWiFS observations and individual model outputs range from $\rho_s = 0.7$ (PISCES) to $\rho_s = 0.1$ (NEMURO), and correlations are low because most models underestimate overall chlorophyll *a* concentrations.

BGD

10, 17193–17247, 2013

Distribution, dominance and ecological niches of PFTs

M. Vogt et al.

Title Page

Abstract

Introduction

Conclusions

References

Tables

Figures

⏪

⏩

◀

▶

Back

Close

Full Screen / Esc

Printer-friendly Version

Interactive Discussion

Distribution, dominance and ecological niches of PFTs

M. Vogt et al.

Title Page

Abstract

Introduction

Conclusions

References

Tables

Figures

⏪

⏩

◀

▶

Back

Close

Full Screen / Esc

Printer-friendly Version

Interactive Discussion

When observed and simulated chlorophyll *a* are compared on a monthly basis, we find that models achieve higher spatial correlation coefficients (Spearman rank correlation coefficient ρ_s) with the observations during the NH summer (June–August; mean: $\bar{\rho}_s = 0.46$, range: 0.35–0.6) than during the NH winter (December–February, mean: $\bar{\rho}_s = 0.38$, range: 0.17–0.59), and that correlations are stronger in NH spring (March–May; mean: $\bar{\rho}_s = 0.42$, range: 0.24–0.65) than in NH autumn (September–November; mean: $\bar{\rho}_s = 0.29$, range: 0.09–0.49). Hence, the model-data agreement is better during the seasons where chlorophyll *a* is high in the NH. All models tend to simulate chlorophyll *a* seasonality better in the high latitudes (North Atlantic and Southern Ocean) than in the low latitudes, where average concentrations and seasonal variability are low. Both the model with the highest (PISCES) and the lowest (CCSM-BEC) absolute chlorophyll *a* concentrations (see Fig. 6) show large areas of high positive temporal correlation ($\rho_t > 0.8$) with observations.

Appendix C

GAM sensitivity tests – model deviances explained

Modelled deviance explained for different combinations of input variables (NO_3 , SST and MLD) are shown in Fig. 7 below.

Acknowledgements. M.V. acknowledges funding from ETH Zurich and EUR-OCEANS. E.T.B. acknowledges funding from EMBRACE (EU contract 282672). M.R.P. would like to acknowledge funding from the Centre of Ocean Life, a VKR center of excellence supported by the Villum foundation. S.C.D., I.L., and S.S. acknowledge support from the Center for Microbial Oceanography Research and Education (C-MORE), an NSF Science and Technology Center (EF-0424599). M.V. would like to thank J. Peloquin, Z. Lachkair, D. Santaren and C. Laufkötter for fruitful discussions.

References

- Alvain, S., Moulin, C., Dandonneau, Y., and Bréon, F. M.: Remote sensing of phytoplankton groups in case I waters from global SeaWiFS imagery, *Deep-Sea Res. Pt. I*, 52, 1989–2004, doi:10.1016/j.dsr.2005.06.015, 2005. 17197, 17201, 17203, 17204, 17209, 17210, 17212, 17214, 17219, 17220
- Alvain, S., Moulin, C., Dandonneau, Y., and Loisel, H.: Seasonal distribution and succession of dominant phytoplankton groups in the global ocean: a satellite view, *Global Biogeochem. Cy.*, 22, GB3001, doi:10.1029/2007GB003154, 2008. 17197, 17201, 17202, 17203, 17211, 17212, 17214, 17216, 17219, 17220
- Alvain, S., Loisel, H., and Dessailly, D.: Theoretical analysis of ocean color radiances anomalies and implications for phytoplankton groups detection in case 1 waters, *Opt. Express*, 20, 1070–1083, doi:10.1364/OE.20.001070, 2012. 17197, 17201, 17202
- Alvain, S., Le Quééré, C., Bopp, L., Racault, M.-F., Beaugrand, G., Dessailly, D., and Buitenhuis, E. T.: Rapid climatic driven shifts of diatoms at high latitudes, *Remote Sens. Environ.*, 132, 195–201, doi:10.1016/j.rse.2013.01.014, 2013. 17220
- Anav, A., Friedlingstein, P., Kidston, M., Bopp, L., Ciais, P., Cox, P., Jones, C., Jung, M., Myrneni, R., and Zhu, Z.: Evaluating the land and ocean components of the global carbon cycle in the CMIP5 Earth System Models, *J. Climate*, 26, 6801–6843, doi:10.1175/JCLI-D-12-00417.1, 2013. 17196
- Anderson, T. R.: Plankton functional type modelling: running before we can walk?, *J. Plankton Res.*, 27, 1073–1081, doi:10.1093/plankt/fbi076, 2005. 17197, 17222
- Aumont, O. and Bopp, L.: Globalizing results from ocean in situ iron fertilization studies, *Global Biogeochem. Cy.*, 20, GB2017, doi:10.1029/2005GB002591, 2006. 17196, 17199, 17200
- Baas Becking, L. G. M.: *Geobiologie of Inleiding Tot de Milieukunde*, W. P. Van Stockum and Zoon, The Hague, the Netherlands, 1934. 17205
- Balch, W., Kilpatrick, K., and Holligan, P.: The 1991 coccolithophore bloom in the central North Atlantic. 2. Relating optics to coccolith concentration, *Limnol. Oceanogr.*, 41, 1684–1696, 1996. 17197, 17203
- Balch, W. M., Gordon, H. R., Bowler, B. C., Drapeau, D. T., and Booth, E. S.: Calcium carbonate measurements in the surface global ocean based on Moderate-Resolution Imaging Spectroradiometer data, *J. Geophys. Res.*, 110, C07001, doi:10.1029/2004JC002560, 2005. 17219

Title Page

Abstract

Introduction

Conclusions

References

Tables

Figures

⏪

⏩

◀

▶

Back

Close

Full Screen / Esc

Printer-friendly Version

Interactive Discussion



Distribution, dominance and ecological niches of PFTs

M. Vogt et al.

Title Page

Abstract

Introduction

Conclusions

References

Tables

Figures

◀

▶

◀

▶

Back

Close

Full Screen / Esc

Printer-friendly Version

Interactive Discussion

- Barton, A. D., Dutkiewicz, S., Flierl, G., Bragg, J., and Follows, M. J.: Patterns of diversity in marine phytoplankton, *Science*, 327, 1509–1511, doi:10.1126/science.1184961, 2010. 17198
- Barton, A. D., Pershing, A. J. E. L., Record, N. R., Edwards, K. F., Finkel, Z. V., Kjørboe, T., and Ward, B. A.: The biogeography of marine plankton traits, *Ecol. Lett.*, 16, 522–534, doi:10.1111/ele.12063, 2013. 17223
- Beaugrand, G. and Helaouët, P.: Simple procedures to assess and compare the ecological niche of species, *Mar. Ecol.-Prog. Ser.*, 363, 29–37, doi:10.3354/meps07402, 2008. 17198
- Beaugrand, G. and Ibanez, F.: Monitoring marine plankton ecosystems. II: Long-term changes in North Sea calanoid copepods in relation to hydro-climatic variability, *Mar. Ecol.-Prog. Ser.*, 284, 35–47, 2004. 17198
- Bopp, L., Kohfeld, K. E., Le Quéré, C., and Aumont, O.: Dust impact on marine biota and atmospheric CO₂ during glacial periods, *Paleoceanography*, 18, 1046, doi:10.1029/2002PA000810, 2003. 17196
- Bopp, L., Aumont, O., Cadule, P., Alvain, S., and Gehlen, M.: Response of diatoms distribution to global warming and potential implications: a global model study, *Geophys. Res. Lett.*, 32, L19606, doi:10.1029/2005GL023653, 2005. 17216, 17218
- Bracher, A., Vountas, M., Dinter, T., Burrows, J. P., Röttgers, R., and Peeken, I.: Quantitative observation of cyanobacteria and diatoms from space using PhytoDOAS on SCIAMACHY data, *Biogeosciences*, 6, 751–764, doi:10.5194/bg-6-751-2009, 2009. 17197, 17203
- Brewin, R. J., Hardman-Mountford, N. J., Lavender, S. J., Raitsos, D. E., Hirata, T., Uitz, J., Devred, E., Bricaud, A., Ciotti, A., and Gentili, B.: An intercomparison of bio-optical techniques for detecting dominant phytoplankton size class from satellite remote sensing, *Remote Sens. Environ.*, 115, 325–339, doi:10.1016/j.rse.2010.09.004, 2011. 17197
- Brown, C. W. and Yoder, J. A.: Coccolithophorid blooms in the global ocean blooms annually covered an average, *J. Geophys. Res.*, 99, 7467–7482, doi:10.1029/93JC02156, 1994. 17197, 17203
- Bruggeman, J. and Kooijman, S. A. L. M.: A biodiversity-inspired approach to aquatic ecosystem modeling, *Limnol. Oceanogr.*, 52, 1533–1544, doi:10.4319/lo.2007.52.4.1533, 2007. 17223
- Buesseler, K.: The decoupling of production and particulate export in the surface ocean, *Global Biogeochem. Cy.*, 12, 297–310, doi:10.1029/97GB03366, 1998. 17215, 17216

Distribution, dominance and ecological niches of PFTs

M. Vogt et al.

Title Page

Abstract

Introduction

Conclusions

References

Tables

Figures

⏪

⏩

◀

▶

Back

Close

Full Screen / Esc

Printer-friendly Version

Interactive Discussion

- Buitenhuis, E., Le Quéré, C., Aumont, O., Beaugrand, G., Bunker, A., Hirst, A., Ikeda, T., O'Brien, T., Piontkovski, S., and Straile, D.: Biogeochemical fluxes through mesozooplankton, *Global Biogeochem. Cy.*, 20, GB2003, doi:10.1029/2005GB002511, 2006. 17198
- 5 Buitenhuis, E., Rivkin, R., Saille, S., and Le Quéré, C.: Biogeochemical fluxes through microzooplankton, *Global Biogeochem. Cy.*, 24, GB4015, doi:10.1029/2009GB003601, 2010. 17197, 17198, 17199
- Buitenhuis, E. T., Hashioka, T., and Le Quéré, C.: Combined constraints on global ocean primary production using observations and models, *Global Biogeochem. Cy.*, 27, 1–12, doi:10.1002/gbc.20074, 2013a. 17196
- 10 Buitenhuis, E. T., Vogt, M., Moriarty, R., Bednaršek, N., Doney, S. C., Leblanc, K., Le Quéré, C., Luo, Y.-W., O'Brien, C., O'Brien, T., Peloquin, J., Schiebel, R., and Swan, C.: MAREDAT: Towards a world atlas of MARine Ecosystem DATA, *Earth Syst. Sci. Data*, 5, 227–239, doi:10.5194/essd-5-227-2013, 2013b. 17197, 17217, 17219, 17221, 17223
- Chase, J. M. and Leibold, M. A.: *Ecological niches: linking classical and contemporary approaches*, The University of Chicago Press, Chicago and London, 2003. 17198
- 15 Cropp, R. A. and Norbury, J.: The mechanisms of coexistence and competitive exclusion in complex plankton ecosystem models, *Ecosystems*, 15, 200–212, doi:10.1007/s10021-011-9503-1, 2012. 17198
- de Boyer Montégut, C., Madec, G., Fischer, A. S., Lazar, A., and Iudicone, D.: Mixed layer depth over the global ocean: an examination of profile data and a profile-based climatology, *J. Geophys. Res.*, 109, C12003, doi:10.1029/2004JC002378, 2004. 17204
- 20 Doney, S., Lima, I., Moore, J. K., Lindsay, K., Behrenfeld, M. J., Westberry, T. K., Mahowald, N., Glover, D. M., and Takahashi, T.: Skill metrics for confronting global upper ocean ecosystem-biogeochemistry models against field and remote sensing data, *J. Marine Syst.*, 76, 95–112, doi:10.1016/j.jmarsys.2008.05.015, 2009. 17222
- Doney, S. C., Ruckelshaus, M., Duffy, J. E., Barry, J. P., Chan, F., English, C. A., Galindo, H. M., Grebmeier, J. M., Hollowed, A. B., Knowlton, N., Polovina, J., Rabalais, N. N., Sydeman, W. J., and Talley, L. D.: Climate change impacts on marine ecosystems, *Annu. Rev. Mar. Sci.*, 4, 11–37, doi:10.1146/annurev-marine-041911-111611, 2012. 17196
- 30 Dupouy, C., Benielli-Gary, D., Neveux, J., Dandonneau, Y., and Westberry, T. K.: An algorithm for detecting *Trichodesmium* surface blooms in the South Western Tropical Pacific, *Biogeosciences*, 8, 3631–3647, doi:10.5194/bg-8-3631-2011, 2011. 17197, 17203

Distribution, dominance and ecological niches of PFTs

M. Vogt et al.

Title Page

Abstract

Introduction

Conclusions

References

Tables

Figures

⏪

⏩

◀

▶

Back

Close

Full Screen / Esc

Printer-friendly Version

Interactive Discussion

- Goldman, J. C.: Potential role of large oceanic diatoms in new primary production, *Deep-Sea Res. Pt. I*, 40, 159–168, doi:10.1016/0967-0637(93)90059-C, 1993. 17215
- Gordon, H. R. and McCluney, W. R.: Estimating the depth of sunlight penetration in the sea for remote sensing, *Appl. Optics*, 14, 413–416, doi:10.1364/AO.14.000413, 1975. 17217
- 5 Hashioka, T. and Yamanaka, Y.: Ecosystem change in the western North Pacific associated with global warming using 3D-NEMURO, *Ecol. Model.*, 202, 95–104, doi:10.1016/j.ecolmodel.2005.12.002, 2007. 17198
- Hashioka, T., Sakamoto, T. T., and Yamanaka, Y.: Potential impact of global warming on North Pacific spring blooms projected by an eddy-permitting 3-D ocean ecosystem model, *Geophys. Res. Lett.*, 36, 1–5, doi:10.1029/2009GL038912, 2009. 17198
- 10 Hashioka, T., Vogt, M., Yamanaka, Y., Le Quéré, C., Buitenhuis, E. T., Aita, M. N., Alvain, S., Bopp, L., Hirata, T., Lima, I., Saille, S., and Doney, S. C.: Phytoplankton competition during the spring bloom in four Plankton Functional Type Models, *Biogeosciences Discuss.*, 9, 18083–18129, doi:10.5194/bgd-9-18083-2012, 2012. 17198, 17201, 17206, 17211, 17218, 17222
- 15 Hirata, T., Hardman-Mountford, N. J., Brewin, R. J. W., Aiken, J., Barlow, R., Suzuki, K., Isada, T., Howell, E., Hashioka, T., Noguchi-Aita, M., and Yamanaka, Y.: Synoptic relationships between surface Chlorophyll-*a* and diagnostic pigments specific to phytoplankton functional types, *Biogeosciences*, 8, 311–327, doi:10.5194/bg-8-311-2011, 2011. 17197, 17201, 17202, 17203, 17204, 17208, 17209, 17210, 17211, 17212, 17214, 17216, 17219, 17220, 17238
- 20 Hutchinson, E.: Concluding remarks, *Cold Spring Harb. Sym.*, 22, 415–427, doi:10.1159/000340002, 1957. 17198, 17205
- Iglesias-Rodríguez, M. D., Brown, C. W., Doney, S. C., Kleypas, J., Kolber, D., Kolber, Z., Hayes, P. K., and Falkowski, P. G.: Representing key phytoplankton functional groups in ocean carbon cycle models: Coccolithophorids, *Global Biogeochem. Cy.*, 16, 1100, doi:10.1029/2001GB001454, 2002. 17196, 17197, 17203, 17219
- 25 Irwin, A. J., Nelles, A. M., and Finkel, Z. V.: Phytoplankton niches estimated from field data, *Limnol. Oceanogr.*, 57, 787–797, doi:10.4319/lo.2012.57.3.0787, 2012. 17198
- 30 Jin, X., Gruber, N., Dunne, J. P., Sarmiento, J. L., and Armstrong, R. A.: Diagnosing the contribution of phytoplankton functional groups to the production and export of particulate organic carbon, CaCO₃, and opal from global nutrient and alkalinity distributions, *Global Biogeochem. Cy.*, 20, 1–17, doi:10.1029/2005GB002532, 2006. 17216

Distribution, dominance and ecological niches of PFTs

M. Vogt et al.

Title Page

Abstract

Introduction

Conclusions

References

Tables

Figures

⏪

⏩

◀

▶

Back

Close

Full Screen / Esc

Printer-friendly Version

Interactive Discussion

- Kalnay, E., Kanamitsu, M., Kistler, R., Collins, W., Deaven, D., Gandin, L., Iredell, M., Saha, S., White, G., Woollen, J., Zhu, Y., Leetmaa, A., Reynolds, R., Chelliah, M., Ebisuzaki, W., Higgins, W., Janowiak, J., Mo, K. C., Ropelewski, C., Wang, J., Jenne, R., and Joseph, D.: The NCEP/NCAR 40-year reanalysis project, *B. Am. Meteorol. Soc.*, 77, 437–471, 1996. 17201
- 5 Kishi, M. J., Kashiwai, M., Ware, D. M., Megrey, B. A., Eslinger, D. L., Werner, F. E., Noguchi-Aita, M., Azumaya, T., Fujii, M., Hashimoto, S., Huang, D., Iizumi, H., Ishida, Y., Kang, S., Kantakov, G. A., Kim, H.-c., Komatsu, K., Navrotsky, V. V., Smith, S. L., Tadokoro, K., Tsuda, A., Yamamura, O., Yamanaka, Y., Yokouchi, K., Yoshie, N., Zhang, J., Zuenko, Y. I., and Zvalinsky, V. I.: NEMURO – a lower trophic level model for the North Pacific marine ecosystem, *Ecol. Model.*, 202, 12–25, doi:10.1016/j.ecolmodel.2006.08.021, 2007. 17199, 17200
- 10 Laufkötter, C., Vogt, M., and Gruber, N.: Long-term trends in ocean plankton production and particle export between 1960–2006, *Biogeosciences Discuss.*, 10, 5923–5975, doi:10.5194/bgd-10-5923-2013, 2013. 17216
- 15 Le Clainche, Y., Vézina, A., Levasseur, M., Cropp, R. A., Gunson, J. R., Vallina, S. M., Vogt, M., Lancelot, C., Allen, J. I., Archer, S. D., Bopp, L., Deal, C., Elliott, S., Jin, M., Malin, G., Schoemann, V., Simó, R., Six, K. D., and Stefels, J.: A first appraisal of prognostic ocean DMS models and prospects for their use in climate models, *Global Biogeochem. Cy.*, 24, GB3021, doi:10.1029/2009GB003721, 2010. 17196
- 20 Le Quééré, C., Harrison, S. P., Prentice, I. C., Buitenhuis, E. T., Aumont, O., Bopp, L., Claustre, H., Cotrim da Cunha, L., Geider, R., Giraud, X., Klaas, C., Kohfeld, K., Legendre, L., Manizza, M., Platt, T., Rivkin, R. B., Sathyendranath, S., Uitz, J., Watson, A. J., and Wolf-Gladrow, D.: Ecosystem dynamics based on plankton functional types for global ocean biogeochemistry models, *Glob. Change Biol.*, 11, 2016–2040, doi:10.1111/j.1365-2486.2005.01004.x, 2005. 17196, 17202, 17215, 17222
- 25 Leblanc, K., Arístegui, J., Armand, L., Assmy, P., Beker, B., Bode, A., Breton, E., Cornet, V., Gibson, J., Gosselin, M.-P., Kopczynska, E., Marshall, H., Pélouquin, J., Piontkovski, S., Poulton, A. J., Quéguiner, B., Schiebel, R., Shipe, R., Stefels, J., van Leeuwe, M. A., Varela, M., Widdicombe, C., and Yallop, M.: A global diatom database – abundance, biovolume and biomass in the world ocean, *Earth Syst. Sci. Data*, 4, 149–165, doi:10.5194/essd-4-149-2012, 2012. 17217
- 30

Distribution, dominance and ecological niches of PFTs

M. Vogt et al.

Title Page

Abstract

Introduction

Conclusions

References

Tables

Figures

◀

▶

◀

▶

Back

Close

Full Screen / Esc

Printer-friendly Version

Interactive Discussion

- Lima, I. D., Lam, P. J., and Doney, S. C.: Dynamics of particulate organic carbon flux in a global ocean model, *Biogeosciences Discuss.*, 10, 14715–14767, doi:10.5194/bgd-10-14715-2013, 2013. 17216
- Litchman, E. and Klausmeier, C. A.: Trait-based community ecology of phytoplankton, *Annu. Rev. Ecol. Evol. S.*, 39, 615–639, doi:10.1146/annurev.ecolsys.39.110707.173549, 2008. 17197
- Litchman, E., Klausmeier, C. A., Schofield, O. M., and Falkowski, P. G.: The role of functional traits and trade-offs in structuring phytoplankton communities: scaling from cellular to ecosystem level, *Ecol. Lett.*, 10, 1170–1181, doi:10.1111/j.1461-0248.2007.01117.x, 2007. 17199
- Luo, Y.-W., Doney, S. C., Anderson, L. A., Benavides, M., Berman-Frank, I., Bode, A., Bonnet, S., Boström, K. H., Böttjer, D., Capone, D. G., Carpenter, E. J., Chen, Y. L., Church, M. J., Dore, J. E., Falcón, L. I., Fernández, A., Foster, R. A., Furuya, K., Gómez, F., Gundersen, K., Hynes, A. M., Karl, D. M., Kitajima, S., Langlois, R. J., LaRoche, J., Letelier, R. M., Marañón, E., McGillicuddy Jr., D. J., Moisaner, P. H., Moore, C. M., Mouriño-Carballido, B., Mulholland, M. R., Needoba, J. A., Orcutt, K. M., Poulton, A. J., Rahav, E., Raimbault, P., Rees, A. P., Riemann, L., Shiozaki, T., Subramaniam, A., Tyrrell, T., Turk-Kubo, K. A., Varela, M., Villareal, T. A., Webb, E. A., White, A. E., Wu, J., and Zehr, J. P.: Database of diazotrophs in global ocean: abundance, biomass and nitrogen fixation rates, *Earth Syst. Sci. Data*, 4, 47–73, doi:10.5194/essd-4-47-2012, 2012. 17219
- Luo, Y.-W., Lima, I. D., Karl, D. M., and Doney, S. C.: Data-based assessment of environmental controls on global marine nitrogen fixation, *Biogeosciences Discuss.*, 10, 7367–7412, doi:10.5194/bgd-10-7367-2013, 2013. 17219, 17220
- Manizza, M., Le Quéré, C., Watson, A. J., and Buitenhuis, E. T.: Ocean biogeochemical response to phytoplankton-light feedback in a global model, *J. Geophys. Res.-Oceans*, 113, C10010, doi:10.1029/2007JC004478, 2008. 17196
- Martin, J.: Glacial-interglacial CO₂ change: the iron hypothesis, *Paleoceanography*, 5, 1–13, doi:10.1029/PA005i001p00001, 1990. 17206
- Martin, J. H., Coale, K. H., Johnson, K. S., Fitzwater, S. E., Gordon, R. M., Tanner, S. J., Hunter, C. N., Elrod, V. A., Nowicki, J. L., Coley, T. L., Barber, R. T., Lindley, S., Watson, A. J., Scoy, K. V., Law, C. S., Liddicoat, M. I., Ling, R., Stanton, T., Stockel, J., Collins, C., Anderson, A., Bidigare, R., Ondrusek, M., Latasa, M., Millero, F. J., Lee, K., Yao, W., Zhang, J. Z., Friederich, G., Sakamoto, C., Chavez, F., Buck, K., Kolber, Z., Greene, R., Falkowski, P., Chisholm, S. W., Hoge, F., Swift, R., Yungel, J., Turner, S., Nightingale, P., Hatton, A.,

Distribution, dominance and ecological niches of PFTs

M. Vogt et al.

Title Page

Abstract

Introduction

Conclusions

References

Tables

Figures

⏪

⏩

◀

▶

Back

Close

Full Screen / Esc

Printer-friendly Version

Interactive Discussion

Liss, P., and Tindale, N. W.: Testing the iron hypothesis in ecosystems of the Equatorial Pacific Ocean, *Nature*, 371, 123–129, doi:10.1038/371123a0, 1994. 17206

Masotti, I., Moulin, C., Alvain, S., Bopp, L., Tagliabue, A., and Antoine, D.: Large-scale shifts in phytoplankton groups in the Equatorial Pacific during ENSO cycles, *Biogeosciences*, 8, 539–550, doi:10.5194/bg-8-539-2011, 2011. 17220

Michaelis, L. and Menten, M. L.: Die Kinetik der Invertinwirkung, *Biochem. Z.*, 49, 333–369, 1913. 17205

Moore, J. K. and Doney, S. C.: Iron availability limits the ocean nitrogen inventory stabilizing feedbacks between marine denitrification and nitrogen fixation, *Global Biogeochem. Cy.*, 21, GB2001, doi:10.1029/2006GB002762, 2007. 17196

Moore, J. K., Doney, S. C., Glover, D. M., and Fung, I. Y.: Iron cycling and nutrient-limitation patterns in surface waters of the World Ocean, *Deep-Sea Res.*, 49, 463–507, doi:10.1016/s0967-0645(01)00109-6, 2002. 17219, 17221

Moore, J. K., Doney, S. C., and Lindsay, K.: Upper ocean ecosystem dynamics and iron cycling in a global three-dimensional model, *Global Biogeochem. Cy.*, 18, GB4028, doi:10.1029/2004GB002220, 2004. 17199, 17200

Moore, J. K., Doney, S. C., Lindsay, K., Mahowald, N., and Michaels, A. F.: Nitrogen fixation amplifies the ocean biogeochemical response to decadal timescale variations in mineral dust deposition, *Tellus B*, 58, 560–572, doi:10.1111/j.1600-0889.2006.00209.x, 2006. 17196

Moore, T. S., Dowell, M. D., and Franz, B. A.: Detection of coccolithophore blooms in ocean color satellite imagery: a generalized approach for use with multiple sensors, *Remote Sens. Environ.*, 117, 249–263, doi:10.1016/j.rse2001.10.001, 2012. 17219

Mouw, C. B., Yoder, J. A., and Doney, S. C.: Impact of phytoplankton community size on a linked global ocean optical and ecosystem model, *J. Marine Syst.*, 89, 61–75, doi:10.1016/j.jmarsys.2011.08.002, 2012. 17196

Nelson, D. M. and Brzezinski, M. A.: Diatom growth and productivity in an oligotrophic midocean gyre: a 3 yr record from the Sargasso Sea near Bermuda, *Limnol. Oceanogr.*, 42, 473–486, 1997. 17217

O'Brien, C. J., Peloquin, J. A., Vogt, M., Heinle, M., Gruber, N., Ajani, P., Andruleit, H., Arístegui, J., Beaufort, L., Estrada, M., Karentz, D., Koczyńska, E., Lee, R., Poulton, A. J., Pritchard, T., and Widdicombe, C.: Global marine plankton functional type biomass distributions: coccolithophores, *Earth Syst. Sci. Data*, 5, 259–276, doi:10.5194/essd-5-259-2013, 2013. 17219

Distribution, dominance and ecological niches of PFTs

M. Vogt et al.

[Title Page](#)

[Abstract](#)

[Introduction](#)

[Conclusions](#)

[References](#)

[Tables](#)

[Figures](#)

[⏪](#)

[⏩](#)

[◀](#)

[▶](#)

[Back](#)

[Close](#)

[Full Screen / Esc](#)

[Printer-friendly Version](#)

[Interactive Discussion](#)

- Peloquin, J., Swan, C., Gruber, N., Vogt, M., Claustre, H., Ras, J., Uitz, J., Barlow, R., Behrenfeld, M., Bidigare, R., Dierssen, H., Ditullio, G., Fernandez, E., Gallienne, C., Gibb, S., Goericke, R., Harding, L., Head, E., Holligan, P., Hooker, S., Karl, D., Landry, M., Letelier, R., Llewellyn, C. A., Lomas, M., Lucas, M., Mannino, A., Marty, J.-C., Mitchell, B. G., Muller-Karger, F., Nelson, N., O'Brien, C., Prezelin, B., Repeta, D., Jr. Smith, W. O., Smythe-Wright, D., Stumpf, R., Subramaniam, A., Suzuki, K., Trees, C., Vernet, M., Wasmund, N., and Wright, S.: The MAREDAT global database of high performance liquid chromatography marine pigment measurements, *Earth Syst. Sci. Data*, 5, 109–123, doi:10.5194/essd-5-109-2013, 2013. 17197, 17217, 17221, 17222
- Popova, E. E., Yool, A., Coward, A. C., Dupont, F., Deal, C., Elliott, S., Hunke, E., Jin, M., Steele, M., and Zhang, J.: What controls primary production in the Arctic Ocean? Results from an intercomparison of five general circulation models with biogeochemistry, *J. Geophys. Res.-Oceans*, 117, C00D12, 1–16, doi:10.1029/2011JC007112, 2012. 17197
- Raitsos, D. E., Lavender, S. J., Maravelias, C. D., Haralabous, J., Richardson, A. J., and Reid, P. C.: Identifying four phytoplankton functional types from space: an ecological approach, *Limnol. Oceanogr.*, 53, 605–613, doi:10.4319/lo.2008.53.2.0605, 2008. 17197
- Sailley, S., Vogt, M., Doney, S. C., Aita, M. N., Bopp, L., Buitenhuis, E. T., Hashioka, T., Lima, I., Le Quéré, C., and Yamanaka, Y.: Comparing food web structures and dynamics across a suite of global marine ecosystem models, *Ecol. Model.*, 261–262, 43–57, doi:10.1016/j.ecolmodel.2013.04.006, 2013. 17198, 17218, 17222, 17223
- Sarmiento, J. L. and Gruber, N. P.: *Ocean Biogeochemical Dynamics*, Princeton University Press, New Jersey, USA, 2006. 17216
- Sathyendranath, S., Stuart, V., Nair, A., Oka, K., Nakane, T., Bouman, H., Forget, M., Maass, H., and Platt, T.: Carbon-to-chlorophyll ratio and growth rate of phytoplankton in the sea, *Mar. Ecol.-Prog. Ser.*, 383, 73–84, doi:10.3354/meps07998, 2009. 17208, 17238
- Shutler, J. D., Land, P. E., Brown, C. W., Findlay, H. S., Donlon, C. J., Medland, M., Snooke, R., and Blackford, J. C.: Coccolithophore surface distributions in the North Atlantic and their modulation of the air-sea flux of CO₂ from 10 years of satellite Earth observation data, *Biogeosciences*, 10, 2699–2709, doi:10.5194/bg-10-2699-2013, 2013. 17197, 17203
- Siddorn, J. R., Allen, J. I., Blackford, J. C., Gilbert, F. J., Holt, J. T., Holt, M. W., Osborne, J. P., Proctor, R., and Mills, D. K.: Modelling the hydrodynamics and ecosystem of the North-West European continental shelf for operational oceanography, *J. Marine Syst.*, 65, 417–429, doi:10.1016/j.jmarsys.2006.01.018, 2007. 17197

Distribution, dominance and ecological niches of PFTs

M. Vogt et al.

[Title Page](#)

[Abstract](#)

[Introduction](#)

[Conclusions](#)

[References](#)

[Tables](#)

[Figures](#)

[⏪](#)

[⏩](#)

[◀](#)

[▶](#)

[Back](#)

[Close](#)

[Full Screen / Esc](#)

[Printer-friendly Version](#)

[Interactive Discussion](#)

- Sigman, D. and Boyle, E.: Glacial/interglacial variations in atmospheric carbon dioxide, *Nature*, 407, 859–869, doi:10.1038/35038000, 2000. 17196
- Smyth, T. J., Tyrrell, T., and Tarrant, B.: Time series of coccolithophore activity in the Barents Sea, from twenty years of satellite imagery, *Geophys. Res. Lett.*, 31, L11302, doi:10.1029/2004GL019735, 2004. 17197, 17203
- Steinacher, M., Joos, F., Frölicher, T. L., Bopp, L., Cadule, P., Cocco, V., Doney, S. C., Gehlen, M., Lindsay, K., Moore, J. K., Schneider, B., and Segschneider, J.: Projected 21st century decrease in marine productivity: a multi-model analysis, *Biogeosciences*, 7, 979–1005, doi:10.5194/bg-7-979-2010, 2010. 17196
- Stow, C. A., Jolliff, J., McGillicuddy, D. J., Doney, S. C., Allen, J. I., Friedrichs, M. A. M., Rose, K. A., and Wallhead, P.: Skill assessment for coupled biological/physical models of marine systems, *J. Marine Syst.*, 76, 4–15, doi:10.1016/j.jmarsys.2008.03.011, 2009. 17222
- Subramaniam, A. and Brown, C.: Detecting *Trichodesmium* blooms in SeaWiFS imagery, *Deep-Sea Res. Pt. II*, 49, 107–121, doi:10.1016/S0967-0645(01)00096-0, 2001. 17197, 17203
- Tagliabue, A., Mtshali, T., Aumont, O., Bowie, A. R., Klunder, M. B., Roychoudhury, A. N., and Swart, S.: A global compilation of dissolved iron measurements: focus on distributions and processes in the Southern Ocean, *Biogeosciences*, 9, 2333–2349, doi:10.5194/bg-9-2333-2012, 2012. 17206, 17221
- Thomas, M. K., Kremer, C. T., Klausmeier, C. A., and Litchman, E.: A global pattern of thermal adaptation in marine phytoplankton, *Science*, 338, 1085–1088, doi:10.1126/science.1224836, 2012. 17197, 17223
- Uitz, J., Claustre, H., Morel, A., and Hooker, S. B.: Vertical distribution of phytoplankton communities in open ocean: an assessment based on surface chlorophyll, *J. Geophys. Res.-Oceans*, 111, C08005, doi:10.1029/2005JC003207, 2006. 17197
- Vogt, M., Vallina, S. M., Buitenhuis, E. T., Bopp, L., and Le Quéré, C.: Simulating dimethylsulphide seasonality with the Dynamic Green Ocean Model PlankTOM5, *J. Geophys. Res.-Oceans*, 115, C06021, 1–21, doi:10.1029/2009JC005529, 2010. 17196
- Wang, S. and Moore, J. K.: Incorporating *Phaeocystis* into a Southern Ocean ecosystem model, *J. Geophys. Res.-Oceans*, 116, C01019, 1–18, doi:10.1029/2009JC005817, 2011. 17197
- Weber, S. N.: *Generalized Additive Models*, Chapman & Hall/CRC, 2006. 17206
- Weber, T. and Deutsch, C.: Ocean nutrient ratios governed by plankton biogeography, *Nature*, 467, 550–554, doi:10.1038/nature09403, 2010. 17196, 17215

Weber, T. and Deutsch, C.: Ocean nitrogen reservoir regulated by plankton diversity and ocean circulation, *Nature*, 489, 418–422, doi:10.1038/nature11357, 2012. 17196, 17215

Westberry, T. K. and Siegel, D. A.: Spatial and temporal distribution of *Trichodesmium* blooms in the world's oceans, *Global Biogeochem. Cy.*, 20, GB4016, doi:10.1029/2005GB002673, 2006. 17197, 17203

5 Yamanaka, Y., Yoshie, N., Fujii, M., Aita, M. N., and Kishi, M. J.: An ecosystem model coupled with nitrogen–silicon–carbon cycles applied to station A7 in the Northwestern Pacific, *J. Oceanogr.*, 60, 227–241, doi:10.1023/B:JOCE.0000038329.91976.7d, 2004. 17199, 17200

BGD

10, 17193–17247, 2013

**Distribution,
dominance and
ecological niches of
PFTs**

M. Vogt et al.

Title Page

Abstract

Introduction

Conclusions

References

Tables

Figures

⏪

⏩

◀

▶

Back

Close

Full Screen / Esc

Printer-friendly Version

Interactive Discussion



Distribution, dominance and ecological niches of PFTs

M. Vogt et al.

Table 1. Characteristics of the Phase-0 models: ecosystem structure, physical model, and references for further reading. pPFTs: phytoplankton functional types, zPFTs: zooplankton functional types.

Model	PlankTOM5	PISCES	CCSM-BEC	NEMURO
pPFTs	diatoms (silicifiers) nanophytoplankton coccolithophores (calcifiers)	diatoms (silicifiers) nanophytoplankton	diatoms (silicifiers) nanophytoplankton diazotrophs (nitrogen fixers)	diatoms (silicifiers) nanophytoplankton
zPFTs	microzooplankton mesozooplankton	microzooplankton mesozooplankton	generic zooplankton	microzooplankton mesozooplankton macrozooplankton
Nutrients	PO ₄ SiO ₃ , Fe	NO ₃ , NH ₄ , PO ₄ SiO ₃ , Fe	NO ₃ , NH ₄ , PO ₄ SiO ₃ , Fe	NO ₃ , NH ₄ SiO ₃ , Fe
Detritus	POM _s , POM _l , DOM CaCO ₃ , SiO ₂	POM _s , POM _l , DOM CaCO ₃ , SiO ₂	POM, DOM CaCO ₃ , SiO ₂	POM, DOM CaCO ₃ , SiO ₂
Physical Model	NEMO	NEMO	CCSM-POP	COCO
Resolution	2° × 0.5–2°	2° × 0.5–2°	3.6° × 0.8–1.8°	1° × 1°
Forcing	NCEP-NCAR	NCEP-NCAR	NCEP-NCAR	NCEP-NCAR
Reference	Buitenhuis et al., 2010	Aumont & Bopp, 2006	Moore et al., 2004	Aita et al., 2007

Title Page

Abstract

Introduction

Conclusions

References

Tables

Figures

⏪

⏩

◀

▶

Back

Close

Full Screen / Esc

Printer-friendly Version

Interactive Discussion

Distribution, dominance and ecological niches of PFTs

M. Vogt et al.

Title Page

Abstract

Introduction

Conclusions

References

Tables

Figures

⏪

⏩

◀

▶

Back

Close

Full Screen / Esc

Printer-friendly Version

Interactive Discussion

Table 2. Global annual mean surface average biomass in mmol C m^{-3} for each pPFT and annual mean surface average chlorophyll *a* in mg Chl m^{-3} for the four models, mean ratio of diatom to nanophytoplankton biomass (D : N ratio), or diatom : total small phytoplankton biomass for the satellite-based estimate (nano-plus picophytoplankton; D : S ratio). ^a Values in brackets indicate chlorophyll equivalents for each PFT in mg Chl m^{-3} . ^b Chlorophyll *a* equivalents in NEMURO and the relative ratio of diatom chlorophyll : nanophytoplankton chlorophyll from Hirata et al. (2011) were converted to/from carbon D : N using a carbon conversion ratio of $50 \text{ g C (g chl)}^{-1}$ for diatoms and a carbon conversion of $125 \text{ g C (g Chl)}^{-1}$ for nano- and picophytoplankton (Sathyendranath et al., 2009).

Model/Biomass	Diatom	Nanophytoplankton	Calcifiers	Diazotrophs	D : N ratio	Total Chl <i>a</i>
PlankTOM5	0.23 (0.05) ^a	1.73 (0.20) ^a	0.21 (0.03) ^a	–	0.12 (0.24) ^a	0.26
PISCES	0.63 (0.14) ^a	1.01 (0.16) ^a	–	–	0.62 (0.88) ^a	0.30
CCSM-BEC	0.41 (0.07) ^a	0.69 (0.09) ^a	–	0.02 (0.004) ^a	0.59 (0.78) ^a	0.17
NEMURO ^b	0.77 (0.07) ^b	0.64 (0.15) ^b	–	–	1.24 (0.47) ^b	0.30
Satellite-derived biomass ^b	Diatoms	Small phytoplankton (Pico- + Nanophytoplankton)	Prymnesiophytes	–	D : S ratio	Chl <i>a</i>
Hirata et al., 2011	0.41 ^b (0.10)	[1.10 + 0.82] ^b (0.11 + 0.08)	0.12 ^b (0.01)	–	0.21 ^b (0.34)	0.30

Distribution, dominance and ecological niches of PFTs

M. Vogt et al.

[Title Page](#)

[Abstract](#)

[Introduction](#)

[Conclusions](#)

[References](#)

[Tables](#)

[Figures](#)

[⏪](#)

[⏩](#)

[◀](#)

[▶](#)

[Back](#)

[Close](#)

[Full Screen / Esc](#)

[Printer-friendly Version](#)

[Interactive Discussion](#)

Table 3. Fraction of $1^\circ \times 1^\circ$ grid cells in % where the different pPFTs are dominant (group constitutes more than 50 % of local biomass) in the annual mean for the four models and two satellite estimates. Coexistence patterns in Hirata et al. (2011) are mostly due to similar proportions of nano- and picophytoplankton.

pPFT/Model	PlankTOM5	PISCES	CCSM-BEC	NEMURO	Alvain et al. (2008)	Hirata et al. (2011)
Silicifiers/Diatoms	9.3	23.0	31.0	36.7	2.2	3.9
Nano-/picophytoplankton	76.8	77.0	68.7	63.3	96.6	76.6
Calcifiers/Prymnesiophytes	12.3	–	–	–	1.2	0.0
Nitrogen fixers	–	–	0.0	–	–	–
Coexistence	1.5	–	0.3	–	–	19.4

Distribution, dominance and ecological niches of PFTs

M. Vogt et al.

[Title Page](#)
[Abstract](#)
[Introduction](#)
[Conclusions](#)
[References](#)
[Tables](#)
[Figures](#)
[Back](#)
[Close](#)
[Full Screen / Esc](#)
[Printer-friendly Version](#)
[Interactive Discussion](#)

Table 4. Model properties: Parameters limiting phytoplankton growth for PlankTOM5, PISCES, CCSM-BEC, NEMURO.

Parameter	PlankTOM5	PISCES	CCSM-BEC	NEMURO
<i>Diatoms:</i>				
$\mu_{\max}(0^\circ\text{C})$	0.6	0.66	0.375	0.8
$f(T)$	1.066^T	1.066^T	$2^{\frac{(T+273.16)-(30+273.15)}{10}}$	$\exp(0.0693 \cdot T)$
$K_{1/2}^{\text{PO}_4}$ (nmol P L ⁻¹)	50.0	4.0	5.0	n/a
$K_{1/2}^{\text{NO}_3}$ (μmol N L ⁻¹)	n/a	1.32	2.5	3.0
$K_{1/2}^{\text{NH}_4}$ (μmol N L ⁻¹)	n/a	0.066	0.08	0.3
$K_{1/2}^{\text{SiO}_3}$ (μmol Si L ⁻¹)	4.0	min: 1.0 (?); max: 7.0 (?)	1.0	6.0
$K_{1/2}^{\text{Fe}}$ (nmol Fe L ⁻¹)	0.12	min: 0.1; max: 0.4	0.15	0.2
<i>Nanophytoplankton:</i>				
$\mu_{\max}(0^\circ\text{C})$	0.4	0.66	0.375	0.4
$f(T)$	1.066^T	1.066^T	$2^{\frac{(T+273.16)-(30+273.15)}{10}}$	$\exp(0.0693 \cdot T)$
$K_{1/2}^{\text{PO}_4}$ (nmol P L ⁻¹)	9.2	0.8	0.3125	n/a
$K_{1/2}^{\text{NO}_3}$ (μmol N L ⁻¹)	n/a	0.26	0.5	1.0
$K_{1/2}^{\text{NH}_4}$ (μmol N L ⁻¹)	n/a	0.013	0.005	0.1
$K_{1/2}^{\text{Fe}}$ (nmol Fe L ⁻¹)	0.04	min: 0.02; max: 0.08	0.06	0.08
<i>Others:</i>				
<i>Coccolithophores</i>		<i>Diazotrophs</i>		
$\mu_{\max}(0^\circ\text{C})$	0.3		0.05	
$f(T)$	1.066^T		$2^{\frac{(T+273.16)-(30+273.15)}{10}}$	
$K_{1/2}^{\text{PO}_4}$ (μmol P L ⁻¹)	0.49		5.0	
$K_{1/2}^{\text{NO}_3}$ (mol N L ⁻¹)	n/a		–	
$K_{1/2}^{\text{NH}_4}$ (mol N L ⁻¹)	n/a		–	
$K_{1/2}^{\text{Fe}}$ (nmol Fe L ⁻¹)	0.07		0.1	

Distribution, dominance and ecological niches of PFTs

M. Vogt et al.

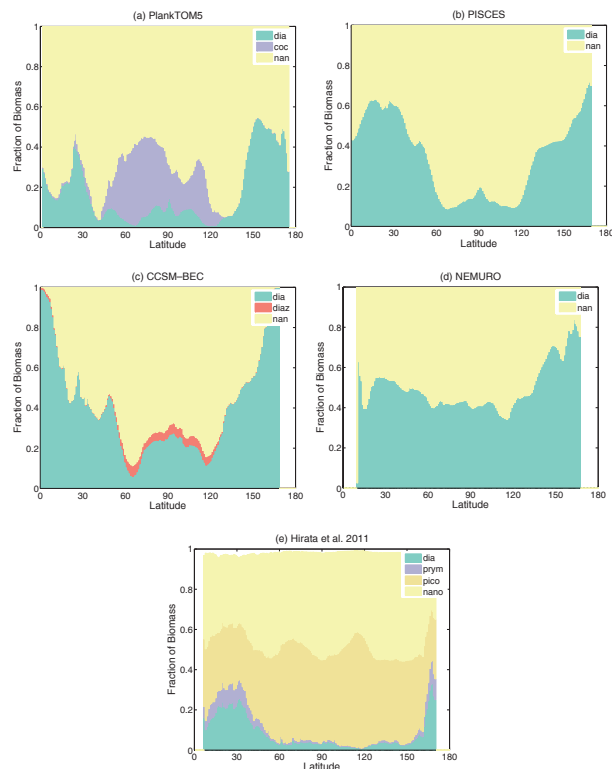


Fig. 1. Comparison of zonal mean surface biomass contributions of the four individual DGOMS to satellite estimates based on Hirata et al. (2011) and conversion factors from Sathyendranath et al. (2009). **(a)** PlankTOM5, **(b)** PISCES, **(c)** NEMURO and **(d)** CCSM-BEC, **(e)** estimates based on Hirata et al. (2011) for all groups resolved by the four models. Legend: dia = diatoms, coc/prym = coccolithophores/prymnesiophytes, diaz = diazotrophs, nano = nanophytoplankton and pico = picophytoplankton.

Title Page

Abstract

Introduction

Conclusions

References

Tables

Figures

◀

▶

◀

▶

Back

Close

Full Screen / Esc

Printer-friendly Version

Interactive Discussion

Distribution, dominance and ecological niches of PFTs

M. Vogt et al.

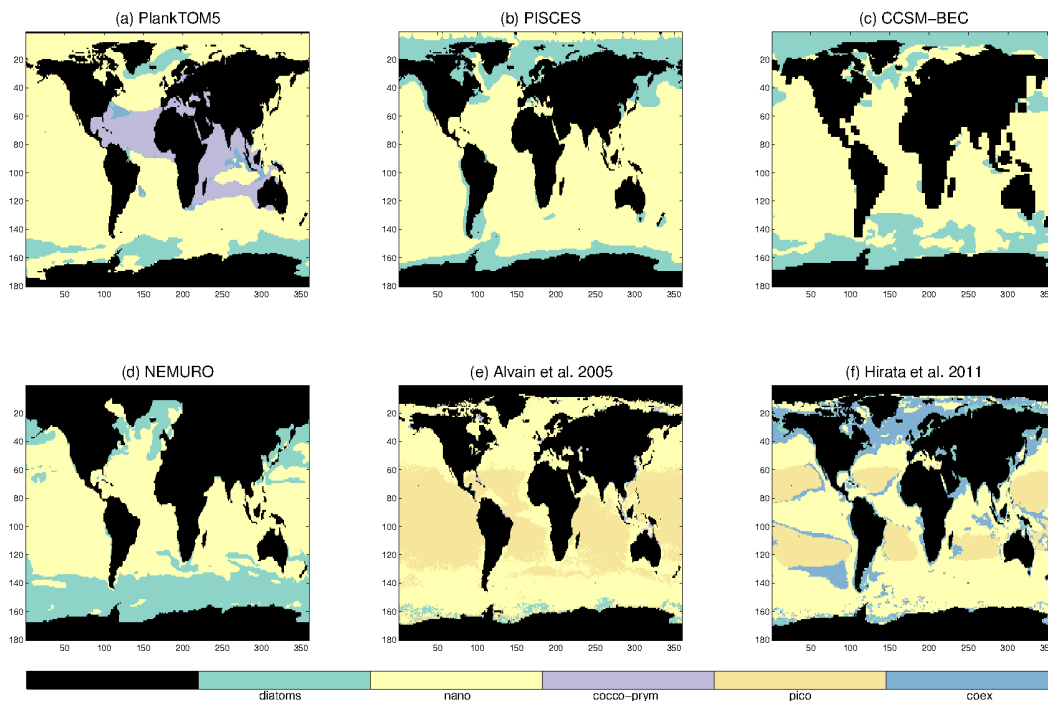


Fig. 2. Annual mean dominance maps for the individual pPFTs **(a)** PlankTOM5, **(b)** for PISCES, **(c)** for NEMURO and **(d)** for CCSM-BEC, as compared to observations from **(e)** PHYSAT (Alvain et al., 2005, 2006, 2008) and **(f)** based on SeaWiFS chlorophyll *a* and the formula in Hirata et al. (2011). Legend: dia = diatoms, cocco-prym = coccolithophores/prymnesiophytes, nano = nanophytoplankton, pico = picophytoplankton. “coex” denotes areas where none of the PFTs constitutes more than 50 % of biomass.

Distribution, dominance and ecological niches of PFTs

M. Vogt et al.

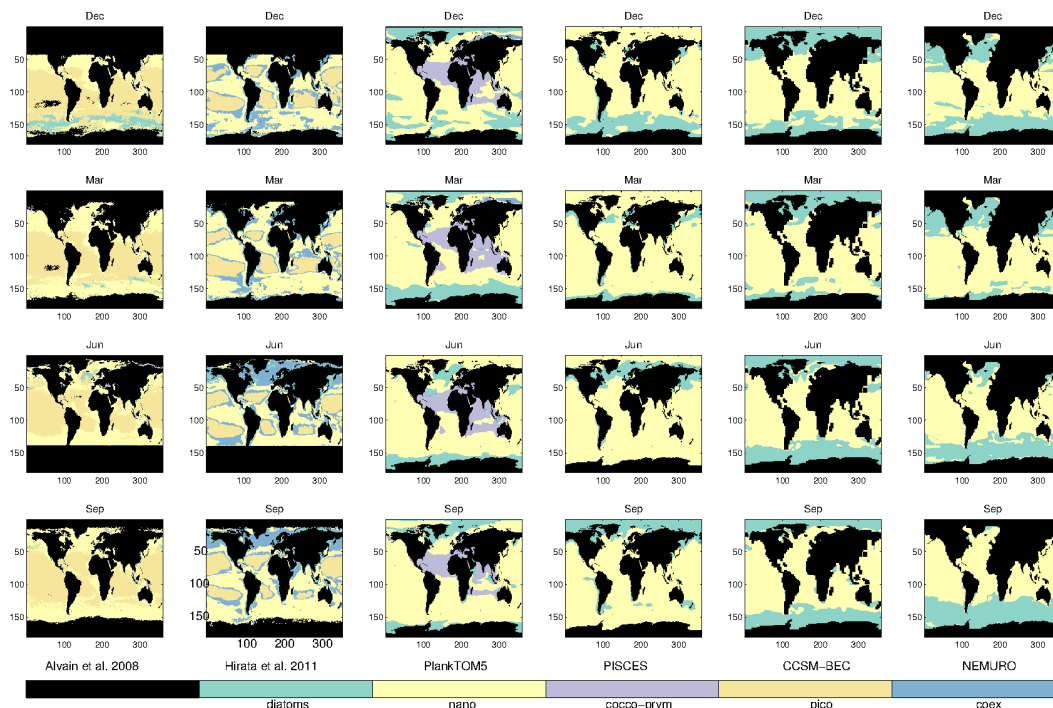


Fig. 3. Monthly mean dominance maps for the individual pPFTs (a) PHYSAT (Alvain et al., 2008), (b) Hirata et al. (2011), (c) PlankTOM5, (d) for PISCES, (e) for NEMURO and (f) for CCSM-BEC for selected Months: December (upper panels), March (upper middle), June (lower middle) and September (lower panels). Legend: dia = diatoms, cocco-prym = coccolithophores/prymnesiophytes, nano = nanophytoplankton, pico = picophytoplankton. “coex” depicts areas where none of the pPFTs is dominant, i.e. none of the pPFTs reaches a biomass contribution of 50%.

[Title Page](#)

[Abstract](#)

[Introduction](#)

[Conclusions](#)

[References](#)

[Tables](#)

[Figures](#)



[Back](#)

[Close](#)

[Full Screen / Esc](#)

[Printer-friendly Version](#)

[Interactive Discussion](#)



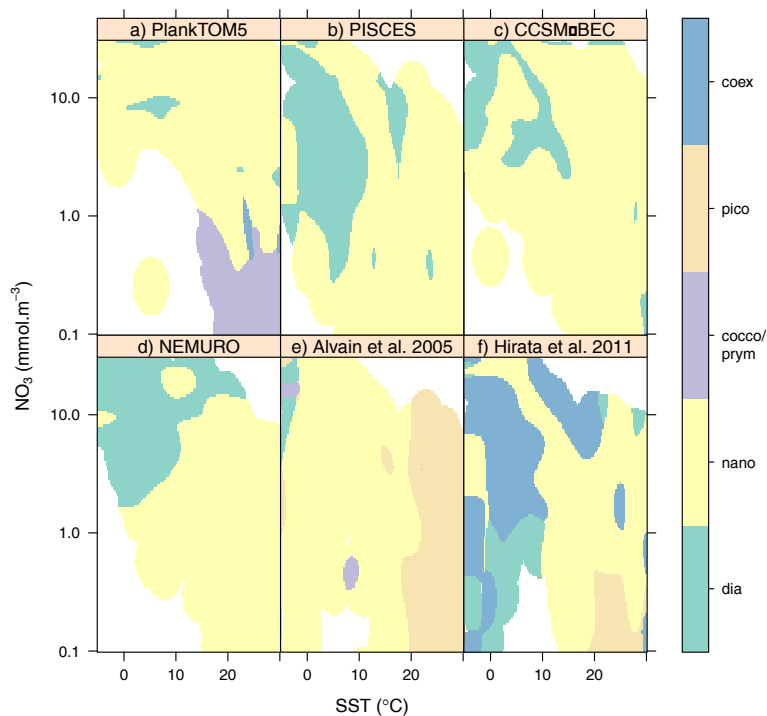


Fig. 4. Representation of dominant pPFT in niche space as pPFT with highest probability of dominance as a function of SST and NO₃ concentration. **(a)** PlankTOM5, **(b)** PISCES, **(c)** CCSM-BEC, **(d)** NEMURO, **(e)** dominance patterns from PHYSAT when only those pPFTs with model equivalents are considered (size classes, diatoms, coccolithophores), and **(f)** dominance patterns from Hirata et al., 2011, where only those pPFTs with model equivalents are considered (size classes, diatoms, prymnesiophytes). Diazotrophs in CCSM-BEC are not dominant in the annual mean. Habitats where none of the pPFTs is dominant, i.e. where no group constitutes more than 50% of biomass, are designated by “coex” Legend as in Figs. 2 and 3.

**Distribution,
dominance and
ecological niches of
PFTs**

M. Vogt et al.

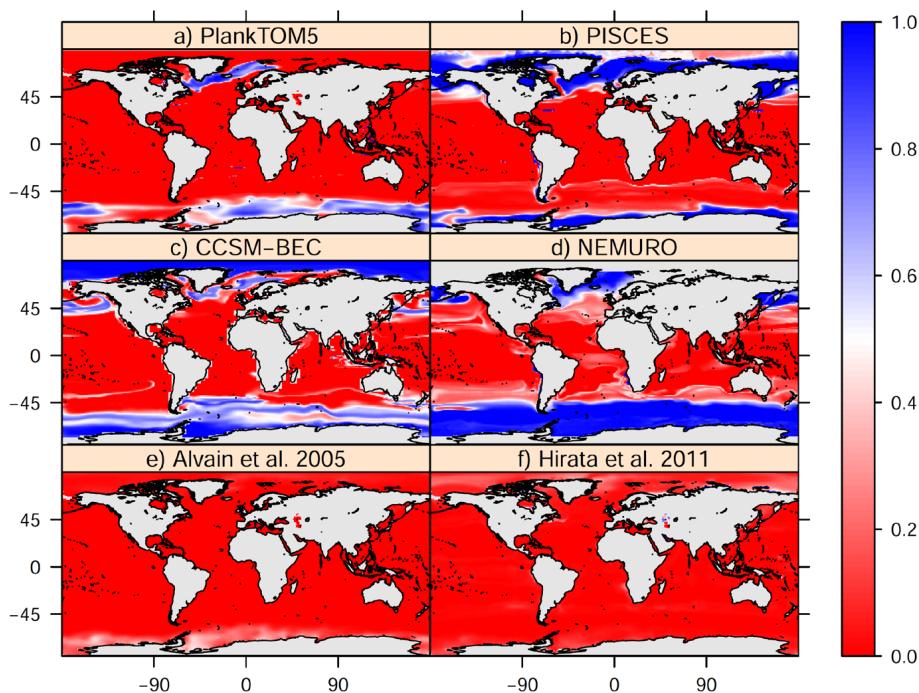


Fig. 5. Global annual mean probability of diatom dominance for the models and the satellite estimates **(a)** PlankTOM5, **(b)** PISCES, **(c)** NEMURO, **(d)** CCSM-BEC **(e)** Alvain et al. (2008), and **(f)** Hirata et al. (2011).

[Title Page](#)[Abstract](#)[Introduction](#)[Conclusions](#)[References](#)[Tables](#)[Figures](#)[◀](#)[▶](#)[◀](#)[▶](#)[Back](#)[Close](#)[Full Screen / Esc](#)[Printer-friendly Version](#)[Interactive Discussion](#)

**Distribution,
dominance and
ecological niches of
PFTs**

M. Vogt et al.

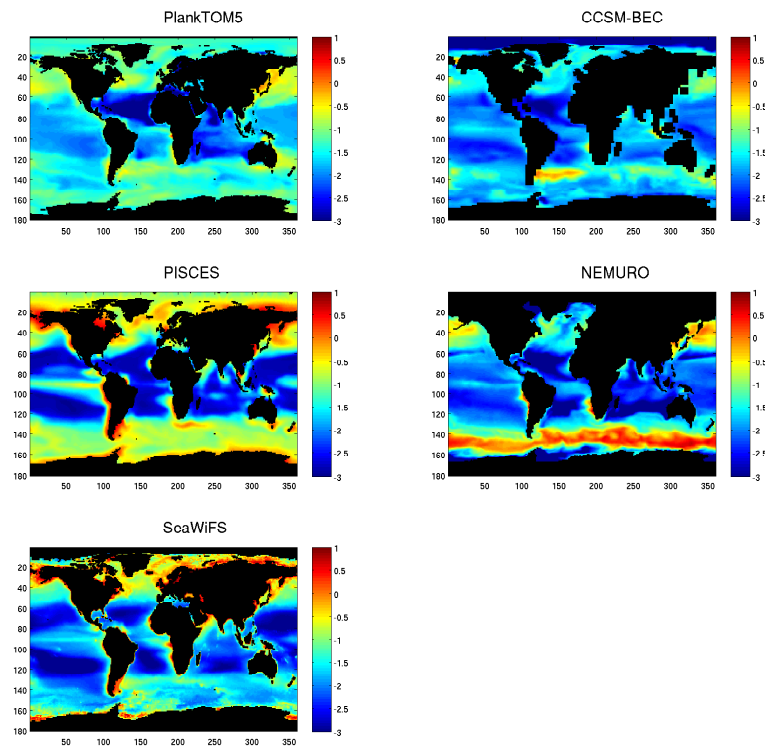


Fig. 6. Log-transformed annual mean chlorophyll *a* for the different DGOMs, as compared to satellite observations: **(a)** PlankTOM5, **(b)** PISCES, **(c)** CCSM-BEC, **(d)** NEMURO, and **(e)** SeaWiFS chlorophyll *a*.

[Title Page](#)[Abstract](#)[Introduction](#)[Conclusions](#)[References](#)[Tables](#)[Figures](#)[Back](#)[Close](#)[Full Screen / Esc](#)[Printer-friendly Version](#)[Interactive Discussion](#)

Distribution, dominance and ecological niches of PFTs

M. Vogt et al.

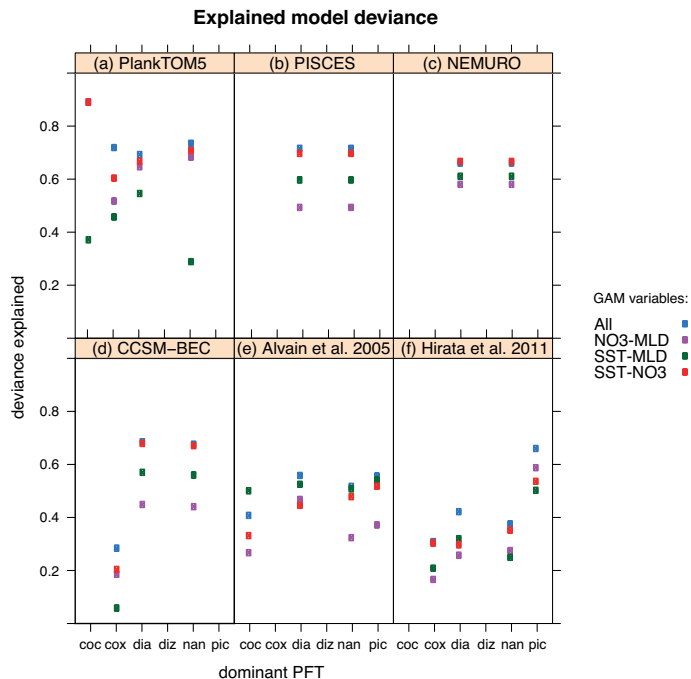


Fig. 7. Explained deviance for the modelled dominance of all plankton functional groups with different combinations as a function of the explanatory variables SST, NO₃ and MLD included in the GAM model for (a) PlankTOM5, (b) PISCES, (c) CCSM-BEC and (d) NEMURO, in comparison to the two satellite estimates (e) Alvain et al. (2005) and (f) Hirata et al. (2011). Modelled variables: coc = coccolihophores, coex = coexistence of several pPFTs, dia = diatoms, diz = diazotrophs, nan = nanophytoplankton, pic = picophytoplankton. Blue dots: all 3 predictor variables included in GAM, violet dots: model with NO₃ and MLD, green: model with SST and MLD and red: model with SST and NO₃. For most pPFTs, differences in the deviance explained are small for the full model (blue), as compared to the reduced model using only SST and NO₃ as predictor variables (red).